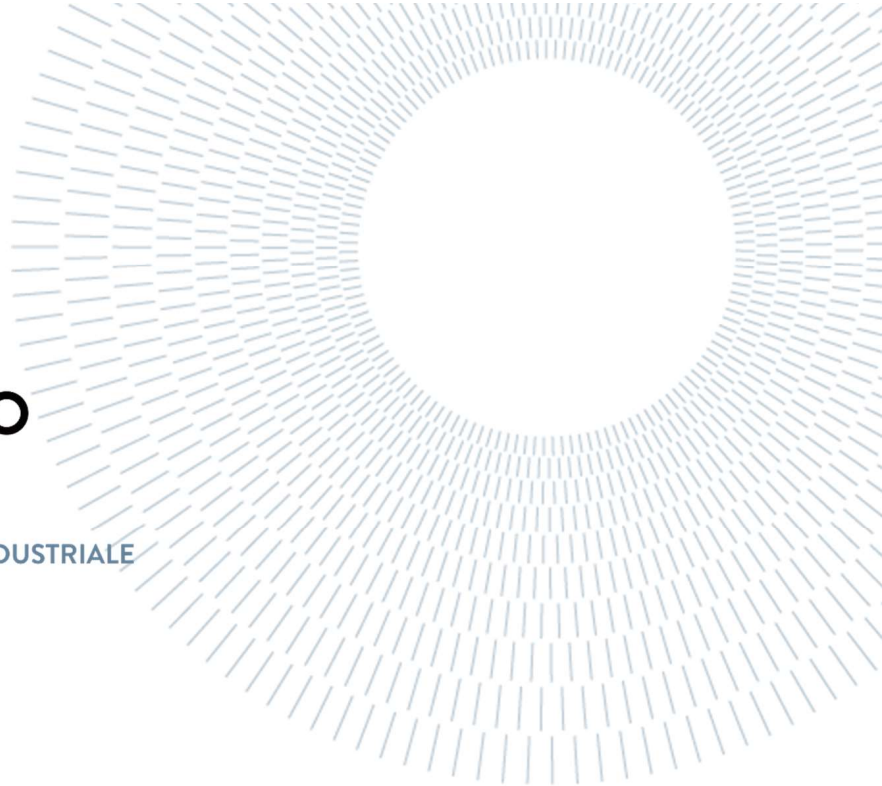




POLITECNICO
MILANO 1863

SCUOLA DI INGEGNERIA INDUSTRIALE
E DELL'INFORMAZIONE



CONTROL OF MECHANICAL SYSTEMS

Course assignments

Mechanical Engineering, Politecnico di Milano

Author:
Lorenzo Vignoli, Student ID: 10712405

Professor: Giuseppe Bucca
Co-professor: Stefano Alfi
Academic Year: 2023-24

Contents

1. Control of a 1-dof mechanical system
 - 1.0. Linearized equation of motion of the system
 - 1.1. Proportional control (P)
 - 1.2. Proportional and derivative control (PD)
 - 1.3. Proportional and integral control (PI)
2. Speed control of a rotor shaft
 - 2.1. CASE A: $kt \rightarrow \infty$
 - 2.2. CASE B: shaft flexibility (torsional spring kt)
3. Control of trajectory of the workpiece of a machine tool
 - 3.1. CASE A: $L_a = 0, kt \rightarrow \infty$.
 - 3.2. CASE B: $L_a \neq 0, kt \rightarrow \infty$.
 - 3.3. CASE C: $L_a = 0, kt = 1000 \text{ Nm/rad}$.

1. Control of a 1-dof mechanical system

1.0. Linearized equation of motion of the system

We focus on the mechanical system shown below:

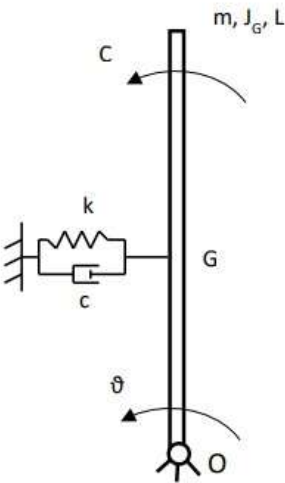


Figure 1: mechanical system

Table 1: system data

Parameter	Value
m [kg]	3
L [m]	4
c [Ns/m]	10
k [N/m]	See Table 2

Table 2: values of stiffness k

Stiffness k	k [N/m]
k_1	150
k_2	Such that the equivalent stiffness $k^* = 0$
k_3	13

Static equilibrium position: $\theta_0 = 0$; C controls the position of the beam. At first, we find the kinematic relationship between physical variables and independent one (θ):

$$v_G = \frac{L}{2} \cdot \dot{\vartheta}$$

$$\omega = \dot{\vartheta}$$

$$\Delta l = \frac{L}{2} \cdot \vartheta \Rightarrow \dot{\Delta l} = \frac{L}{2} \cdot \dot{\vartheta}$$

$$h_G = \frac{L}{2} \cdot \cos\vartheta$$

Energy quantities will be:

$$\delta \mathcal{L} = C \cdot \delta \vartheta$$

$$E_k = \frac{1}{2} m \cdot v_G^2 + \frac{1}{2} J_G \cdot \omega^2 = \frac{1}{2} \left(m \frac{L^2}{4} + J_G \right) \dot{\vartheta}^2 = \frac{1}{2} \cdot m^* \cdot \dot{\vartheta}^2$$

$$D = \frac{1}{2} C \cdot \dot{\Delta l}^2 = \frac{1}{2} \left(C \cdot \frac{L^2}{4} \right) \cdot \dot{\vartheta}^2 = \frac{1}{2} \cdot c^* \cdot \dot{\vartheta}^2$$

$$V = V_{el} + V_g = \frac{1}{2} k \cdot \Delta l^2 + m \cdot g \cdot h_G = \frac{1}{2} \cdot k \cdot \frac{L^2}{4} \vartheta^2 + m \cdot g \cdot \frac{L}{2} \cos\vartheta$$

From Taylor's expansion (note that $\bar{\theta} = \theta - \theta_0 = \theta$):

$$V_g \cong V_g(\theta_0) + \frac{\partial V_g}{\partial \theta} \Big|_{\theta=\theta_0} \cdot (\theta - \theta_0) + \frac{1}{2} \cdot \frac{\partial^2 V_g}{\partial \theta^2} \Big|_{\theta=\theta_0} \cdot (\theta - \theta_0)^2$$

First (constant) term will disappear in the derivation; second one simplifies because of the equilibrium position:

$$\frac{\partial V_g}{\partial \theta} |_{\theta=\theta_0} = C(\theta_0)$$

Then we find that, eliminating the terms that will disappear:

$$V_g \cong \frac{1}{2} \cdot k_{eq} \cdot (\theta - \theta_0)^2 = \frac{1}{2} \cdot (-mg \frac{L}{2}) \cdot \theta^2$$

Using Lagrange equation:

$$\begin{aligned} \frac{d}{dt} \left(\frac{\partial E_k}{\partial \dot{\vartheta}} \right) - \frac{\partial E_k}{\partial \vartheta} + \frac{\partial D}{\partial \dot{\vartheta}} + \frac{\partial V}{\partial \vartheta} &= Q_\theta \\ (m \cdot \frac{L^2}{4} + J_G) \cdot \ddot{\vartheta} + c \cdot \frac{L^2}{4} \cdot \dot{\vartheta} + (k \cdot \frac{L^2}{4} - mg \frac{L}{2}) \cdot \theta &= C \\ m^* \cdot \ddot{\vartheta} + c^* \cdot \dot{\vartheta} + k^* \cdot \vartheta &= C \end{aligned}$$

To characterize the system, we can rely on the state-space form:

$$\begin{aligned} \begin{cases} m^* \cdot \ddot{\vartheta} + c^* \cdot \dot{\vartheta} + k^* \cdot \vartheta = C \\ \dot{\vartheta} = \dot{\vartheta} \end{cases} \\ \begin{bmatrix} m^* & 0 \\ 0 & 1 \end{bmatrix} \cdot \begin{pmatrix} \ddot{\vartheta} \\ \dot{\vartheta} \end{pmatrix} + \begin{bmatrix} c^* & k^* \\ -1 & 0 \end{bmatrix} \cdot \begin{pmatrix} \dot{\vartheta} \\ \vartheta \end{pmatrix} = \begin{pmatrix} 1 \\ 0 \end{pmatrix} \cdot C \\ P = \begin{bmatrix} m^* & 0 \\ 0 & 1 \end{bmatrix}, \quad Q = \begin{bmatrix} c^* & k^* \\ -1 & 0 \end{bmatrix}, \quad N = \begin{pmatrix} 1 \\ 0 \end{pmatrix}, \quad \underline{x} = \begin{pmatrix} \dot{\vartheta} \\ \vartheta \end{pmatrix} \\ A = -P^{-1} \cdot Q, \quad B = P^{-1} \cdot N, \quad u = C \end{aligned}$$

Thus, we get: $\dot{\underline{x}} = A \cdot \underline{x} + B \cdot u$

Eigenvalues of A determine the system's stability: $\det(\lambda \cdot I - A) = 0$, from which we get: $\lambda_{1,2} = -\frac{c^*}{2m^*} \pm \sqrt{\left(\frac{c^*}{2m^*}\right)^2 - \frac{k^*}{m^*}} = -\alpha \pm i \cdot \omega_d$. The uncontrolled system can be subjected to three cases:

- 1) $k^* > 0$: asymptotically stable
- 2) $k^* = 0$: stable
- 3) $k^* < 0$: statically unstable

1.1. Proportional control (P)

It is required to discuss stability and performances (step response: $\vartheta_{ref} = \overline{\vartheta_{ref}}$ · $step(t)$) of the system in time and Laplace domain for increasing values of the proportional gain k_p , considering the three values of stiffness k in Table 2.

$$u = C = k_p \cdot (\vartheta_{ref} - \vartheta)$$

- 1) $k_1 = 150 \text{ N/m}$ (*asymptotically stable case*).

$$k^* = (k \cdot \frac{L^2}{4} - mg \frac{L}{2}) = 541.14 \text{ Nm} > 0$$

Equation of motion of the system becomes: $m^* \cdot \ddot{\vartheta} + c^* \cdot \dot{\vartheta} + (k^* + k_p) \cdot \vartheta = k_p \cdot \vartheta_{ref}$. Using the state-space form method in the same way, we get:

$$\lambda_{1,2} = -\frac{c^*}{2m^*} \pm \sqrt{\left(\frac{c^*}{2m^*}\right)^2 - \frac{k^* + k_p}{m^*}} = -\alpha \pm i \cdot \tilde{\omega}_d$$

$\tilde{\omega}_d > \omega_d$ due to the presence of k_p , while for the same reason $\tilde{h} < h^*$: system is faster, but damping factor gets smaller. Being the system already stable, the introduction of a P control only preserves this stability.

Let's analyze now the system's performances in time domain: solution can be found analytically, solving the ODE and setting initial position and velocity as null:

$$\vartheta(t) = \frac{k_p}{k^* + k_p} \cdot \overline{\vartheta_{ref}} \cdot \left[1 - e^{-\alpha t} \left(\cos \tilde{\omega}_d t + \frac{\alpha}{\tilde{\omega}_d} \cdot \sin \tilde{\omega}_d t \right) \right]$$

i. Steady-state error (e_∞):

$$e_\infty = \theta_{ref} - \theta_\infty = \theta_{ref} \cdot \frac{k^*}{k^* + k_p}$$

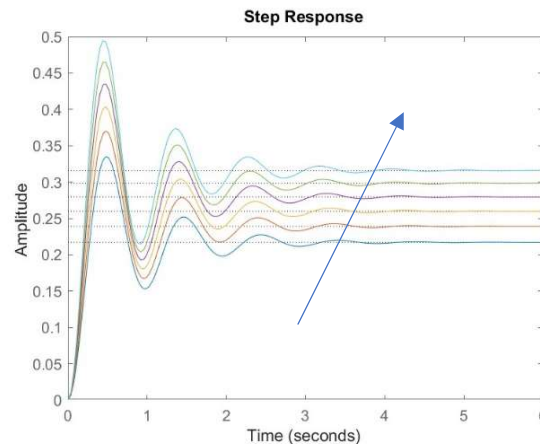


Figure 2: step response (case 1)

ii. Percentage overshoot (P.O.):

$$t_p = \frac{\pi}{\tilde{\omega}_d} \Rightarrow P.O. = \frac{\theta_{max} - \theta_\infty}{\theta_\infty} = e^{-\pi \cdot \tilde{h} / \sqrt{1 - \tilde{h}^2}}$$

If k_p increases, PO increases accordingly (since \tilde{h} decreases). Function `stepinfo()` on MatLab has been used to find these values.

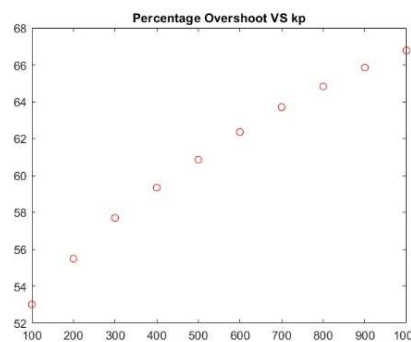


Figure 3: overshoot (case 1)

iii. Rise time (t_r):

Theoretically: $\theta(t = t_r) = 0.9 \cdot \theta_\infty$. We could approximate by considering $\theta(t = t_r) \approx \theta_\infty$, thus getting:

$$t_r = \frac{\pi + \arctan(-\tilde{\omega}_d/\alpha)}{\tilde{\omega}_d}$$

If k_p increases, $\tilde{\omega}_d$ increases reducing t_r . Using *stepinfo()* on MatLab:

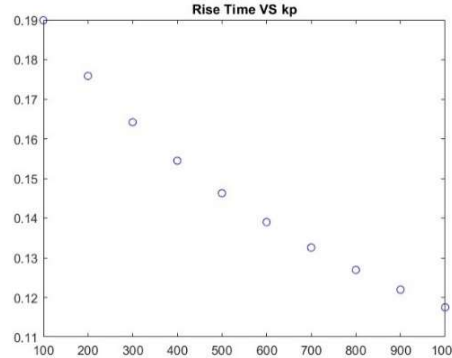


Figure 4: rise time (case 1)

iv. Settling time (t_s):

We could compute it with envelope curves: $\theta_E(t) = \frac{k_p}{k^*+k_p} \cdot \overline{\theta_{ref}} \cdot \left[1 \pm \frac{e^{-\alpha t}}{\sqrt{1-\tilde{h}^2}} \right]$.

This means that:

$$5\% = \frac{e^{-\alpha t_s}}{\sqrt{1-\tilde{h}^2}}$$

Consequently, k_p has a slight relevance on t_s (no relevant trend):

$$t_s = \frac{-\ln(0.05) + 1/2 \cdot \ln(1 - \tilde{h}^2)}{\alpha}$$

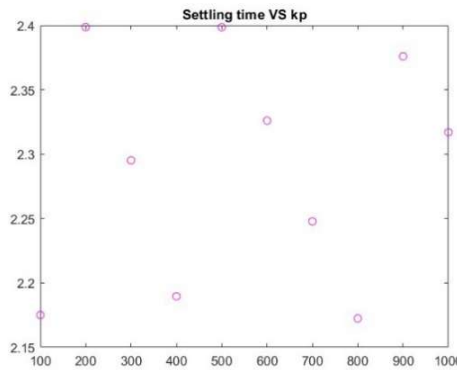


Figure 5: settling time (case 1)

Let's analyze now stability in Laplace domain.

$$GH(s) = \frac{k_p}{m^* \cdot s^2 + c^* \cdot s + k^*} \Rightarrow L(s) = \frac{k_p}{m^* \cdot s^2 + c^* \cdot s + k^* + k_p}$$

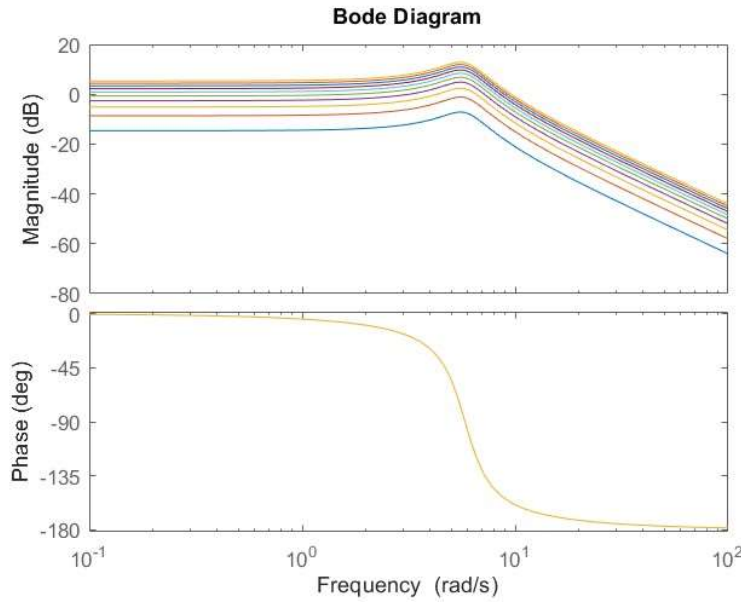


Figure 6: Bode diagram (case 1)

System is minimum phase (uncontrolled system is stable), so Bode criterion can be applied (when diagram is crossing the 0 dB line); phase margin is always positive, thus controlled system is positive $\forall k_P$.

Same can be found using Nyquist criterion; $GH(s)$ has no unstable poles, then no encirclements (neither clockwise nor counterclockwise) around $(-1; 0)$ are allowed for stability. This is verified.

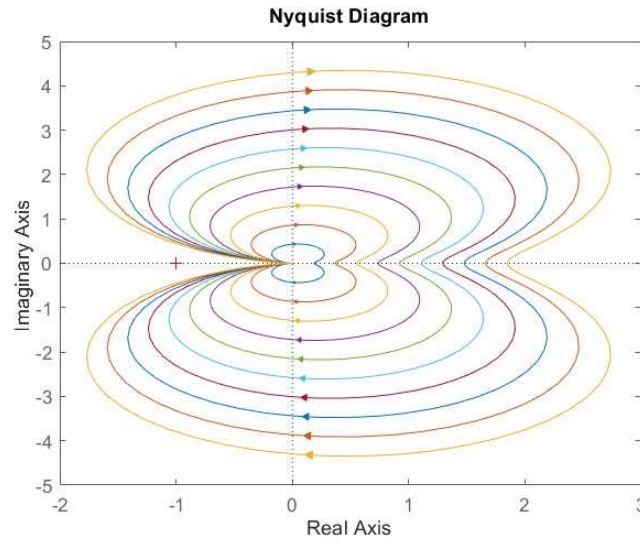


Figure 7: Nyquist diagram (case 1)

Finally, root locus cannot have positive real part to be stable for every value of k_P , and all poles lie on the left-half of the plane.

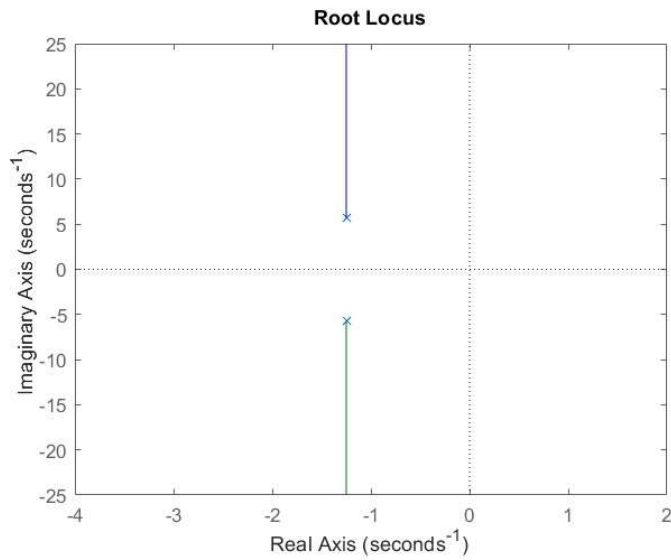


Figure 8: root locus (case 1)

2) $k_2 = 14.715 \text{ N/m}$ (stable case).

To get k_2 : $k^* = (k_2 \cdot \frac{L^2}{4} - mg \frac{L}{2}) = 0 \Rightarrow k_2 = 14.715 \text{ N/m}$.

In this case: $\lambda_1 = 0$, while $\lambda_2 = -\frac{c^*}{m^*} = -2\alpha$.

Performances:

i. Steady-state error (e_∞):

Since k^* is null: $\theta_\infty = \overline{\theta_{ref}} \Rightarrow e_\infty = \theta_{ref} - \theta_\infty = 0 \quad \forall k_p$

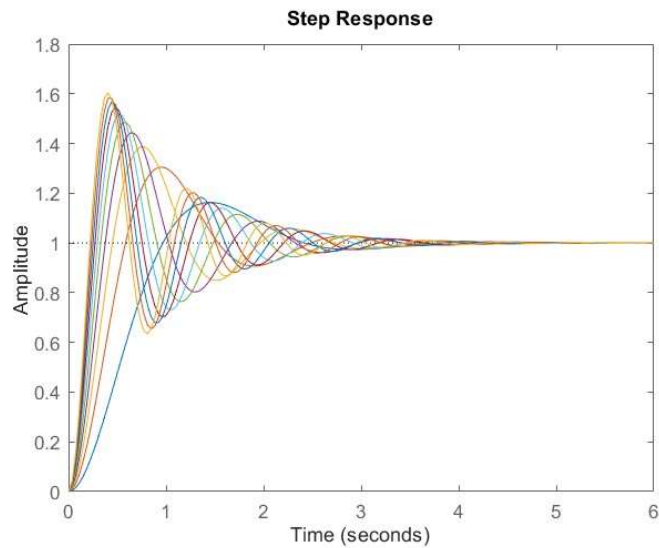


Figure 9: step response (case 2)

ii. Percentage overshoot (P.O.):

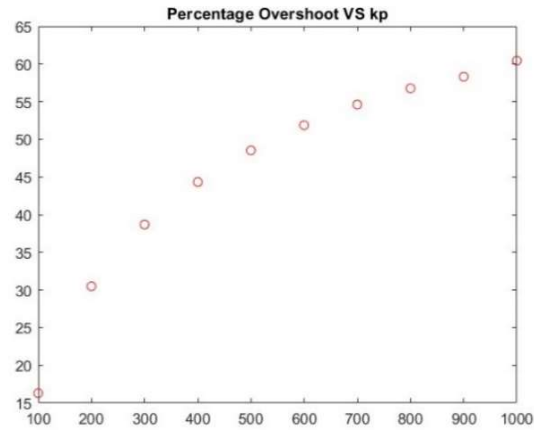


Figure 10: overshoot (case 2)

iii. Rise time (t_r):

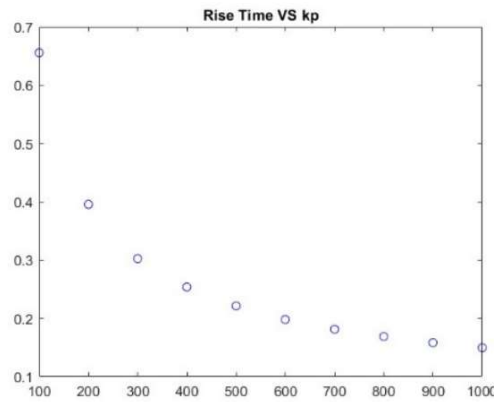


Figure 11: rise time (case 2)

iv. Settling time (t_s):

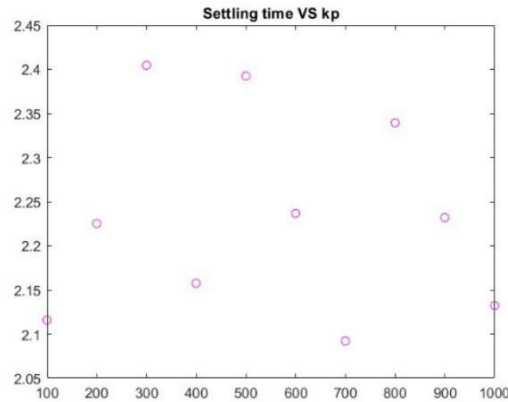


Figure 12: settling time (case 2)

In Laplace domain:

$$GH(s) = \frac{k_P}{m * s^2 + c * s} \Rightarrow L(s) = \frac{k_P}{m * s^2 + c * s + k_P}$$

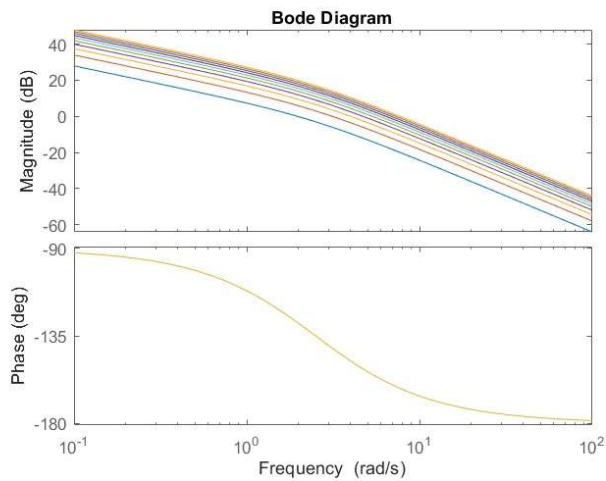


Figure 13: Bode diagram (case 2)

The trend at the beginning highlights the presence of the pole at the origin (which is the reason why there's no steady-state error). Bode criterion can be applied, since GH has no poles with positive real part: for whatever value of k_p system is stable ($P_m > 0$).

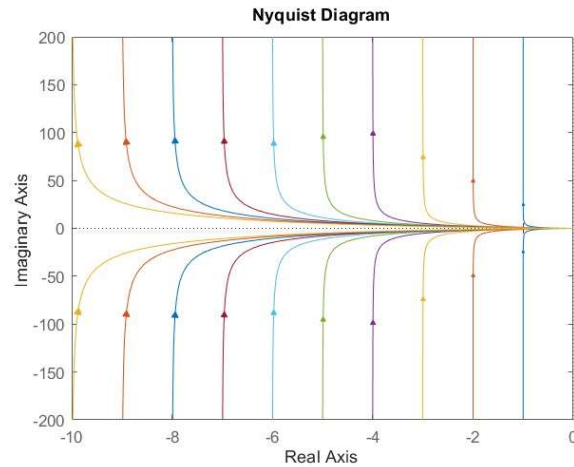


Figure 14: Nyquist diagram (case 2)

No unstable poles of GH and no encirclements around $(-1; 0)$: system's always stable.

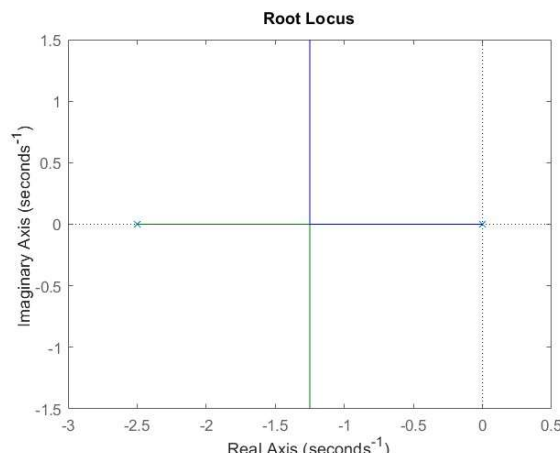


Figure 15: root locus (case 2)

3) $k_3 = 13 \text{ N/m}$ (*unstable case*).

In this case: $\lambda_1 = -\alpha_1$, while $\lambda_2 = \alpha_2$ (with $\alpha_1 > \alpha_2$); $k^* < 0$. Performances:

- i. Steady-state error (e_∞):

$$\theta_\infty = \theta_{ref} \cdot \frac{k_p}{k^* + k_p} > \theta_\infty \Rightarrow e_\infty = \theta_{ref} - \theta_\infty < 0$$

If k_p increases, e_∞ (in absolute value) decreases (obviously, only if controlled system's stable: we only plotted those cases).

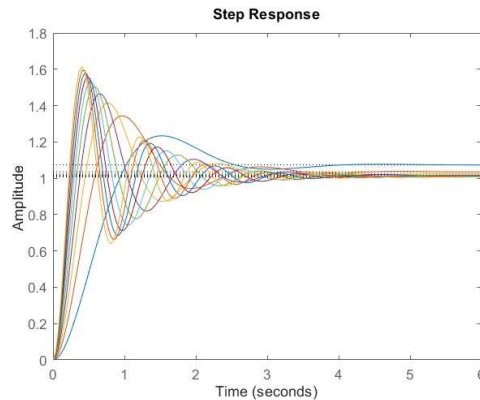


Figure 16: step response (case 3)

- ii. Percentage overshoot (P.O.):

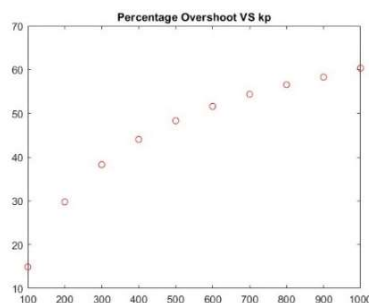


Figure 17: overshoot (case 3)

- iii. Rise time (t_r):

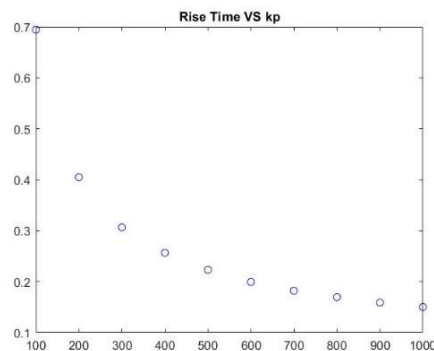


Figure 18: rise time (case 3)

iv. Settling time (t_s):

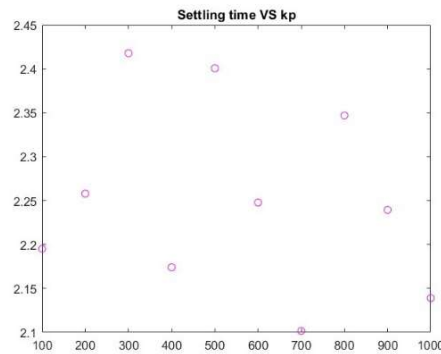


Figure 19: settling time (case 3)

In Laplace domain:

$$GH(s) = \frac{k_p}{m^* \cdot s^2 + c^* \cdot s + k^*} \Rightarrow L(s) = \frac{k_p}{m^* \cdot s^2 + c^* \cdot s + k^* + k_p}$$

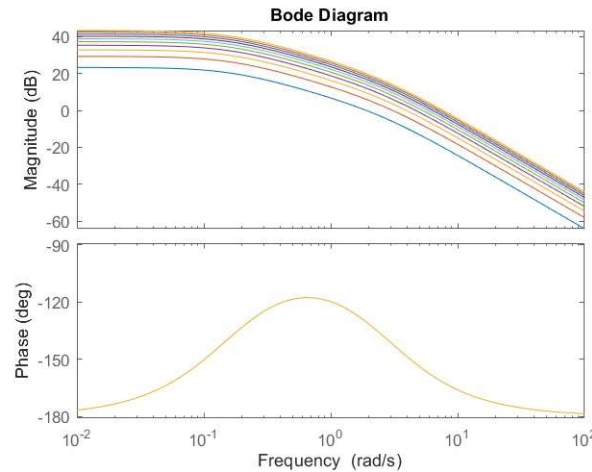


Figure 20: Bode diagram (case 3)

Bode diagram cannot be used to determine instability here, because $GH(s)$ is not minimum phase (one unstable pole). From Nyquist diagram instead:

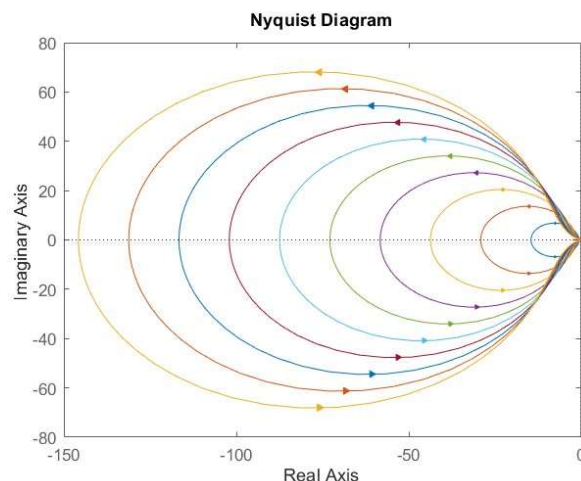


Figure 21: Nyquist diagram (case 3)

One counterclockwise encirclement around (-1; 0) occurs, as one in the number of unstable poles; the system is (for these values of k_p) therefore stable. If k_p would have been lower (e.g. almost negligible), the controlled system wouldn't have been stable due to no encirclements; this is well-visible from the root locus:

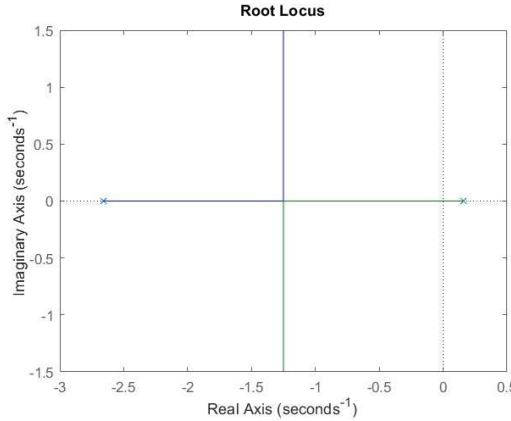


Figure 22: root locus (case 3)

1.2. Proportional and derivative control (PD)

Equation of the controlled system is:

$$m^* \cdot \ddot{\vartheta} + c^* \cdot \dot{\vartheta} + k^* \cdot \vartheta = C = k_p \cdot (\vartheta_{ref} - \vartheta) + k_d \cdot (\dot{\vartheta}_{ref} - \dot{\vartheta})$$

In the state-space form:

$$\begin{cases} m^* \cdot \ddot{\vartheta} + (c^* + k_d) \cdot \dot{\vartheta} + (k^* + k_p) \cdot \vartheta = k_p \cdot \theta_{ref} + k_d \cdot \dot{\theta}_{ref} \\ \dot{\vartheta} = \dot{\vartheta} \end{cases}$$

$$\begin{bmatrix} m^* & 0 \\ 0 & 1 \end{bmatrix} \cdot \begin{pmatrix} \ddot{\vartheta} \\ \dot{\vartheta} \end{pmatrix} + \begin{bmatrix} c^* + k_d & k^* + k_p \\ -1 & 0 \end{bmatrix} \cdot \begin{pmatrix} \dot{\vartheta} \\ \vartheta \end{pmatrix} = \begin{bmatrix} k_d & k_p \\ 0 & 0 \end{bmatrix} \cdot \begin{pmatrix} \dot{\vartheta}_{ref} \\ \vartheta_{ref} \end{pmatrix}$$

$$P = \begin{bmatrix} m^* & 0 \\ 0 & 1 \end{bmatrix}, \quad Q = \begin{bmatrix} c^* + k_d & k^* + k_p \\ -1 & 0 \end{bmatrix};$$

$$N = \begin{bmatrix} k_d & k_p \\ 0 & 0 \end{bmatrix}, \quad \underline{x} = \begin{pmatrix} \dot{\vartheta} \\ \vartheta \end{pmatrix}, \quad \underline{x}_{ref} = \begin{pmatrix} \dot{\vartheta}_{ref} \\ \vartheta_{ref} \end{pmatrix}.$$

$$A = -P^{-1} \cdot Q, \quad B = P^{-1} \cdot N.$$

Thus, we get: $\dot{\underline{x}} = A \cdot \underline{x} + B \cdot \underline{x}_{ref}$: poles are the eigenvalues of A.

1) $k_1 = 150 \text{ N/m}$.

We vary k_D and k_p separately, with $k_p = 100:100:1000$ (while $k_D = 15$) and then $k_D = 100:100:1500$ (while $k_p = 1000$). However, other tunings have been tried to check the parameters' behavior. Resulting performances:

i. Steady-state error (e_∞):

$$e_\infty = \theta_{ref} - \theta_\infty = \theta_{ref} \cdot \frac{k^*}{k^* + k_p}$$

It only depends on k_p , so whatever change in T_D doesn't affect the error.

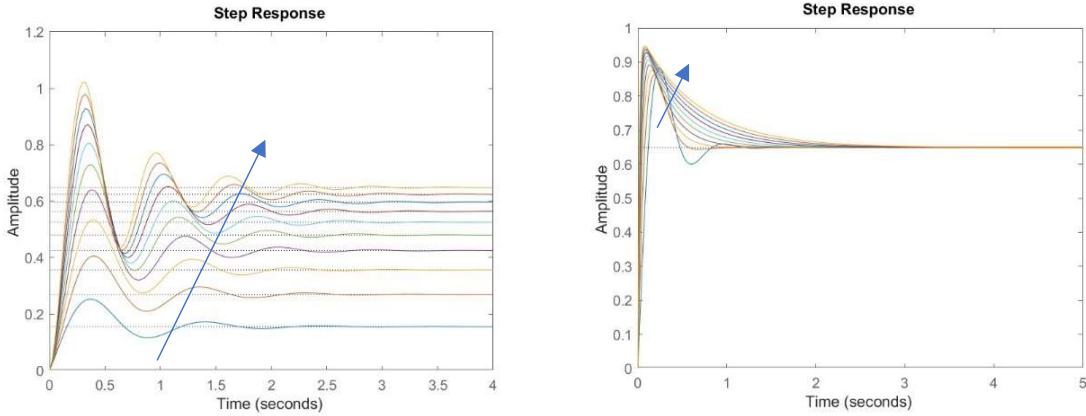


Figure 23: step response, fixed kd or k_p (case 1)

From the step response we can see steady-state response (thus steady-state error) doesn't depend on k_D . The influence on other performances, visible in the graphs, is *strongly* affected by the choice of the parameters: we can identify typical trends for some values, but this won't be always valid for whatever range we choose.

ii. Percentage overshoot (P.O.):

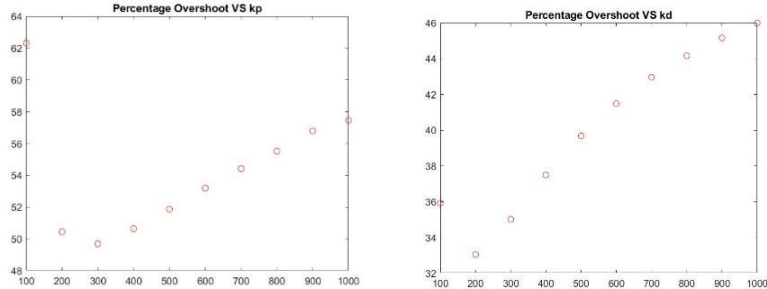


Figure 24: overshoot, fixed kd or k_p (case 1)

If k_p increases, overshoot increases too; if k_D increases, overshoot decreases for small values (and increases for high ones). However, this depends on the parameters' tuning, as shown by the non-monotonous behavior for low k_p and high k_D .

iii. Rise time (t_r):

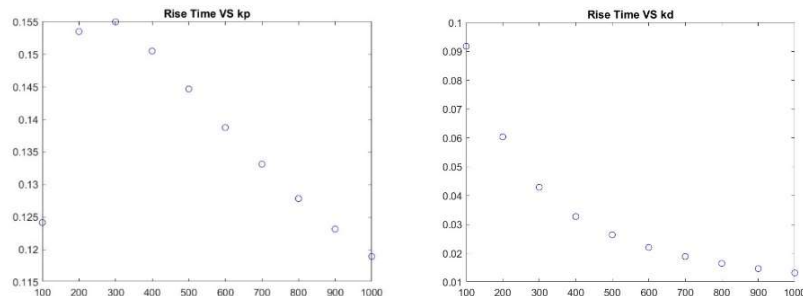


Figure 25: rise time, fixed kd or k_p (case 1)

It decreases for an increase of both k_p and k_D : this will influence behavior more than damping for high values of derivative gain.

iv. Settling time (t_s):

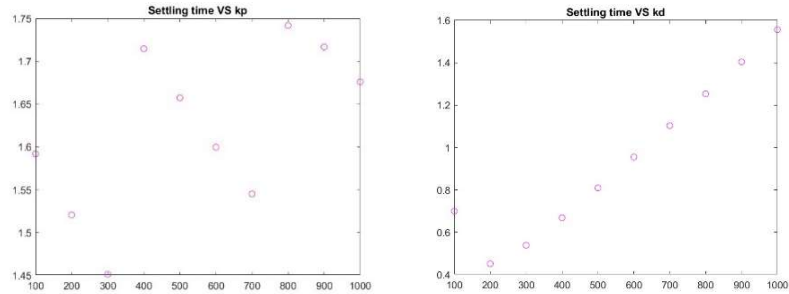


Figure 26: settling time, fixed td or tp (case 1)

There is no effect in varying k_p , while lowering k_d decreases t_s for small values (same eigenfrequency, but higher damping ratio) and increases it for higher ones. In Laplace domain:

$$GH(s) = \frac{k_p + k_d \cdot s}{m^* \cdot s^2 + c^* \cdot s + k^*} \Rightarrow L(s) = \frac{k_p + k_d \cdot s}{m^* \cdot s^2 + (c^* + k_d) \cdot s + k^* + k_p}$$

System is minimum phase, so we can apply Bode criterion.

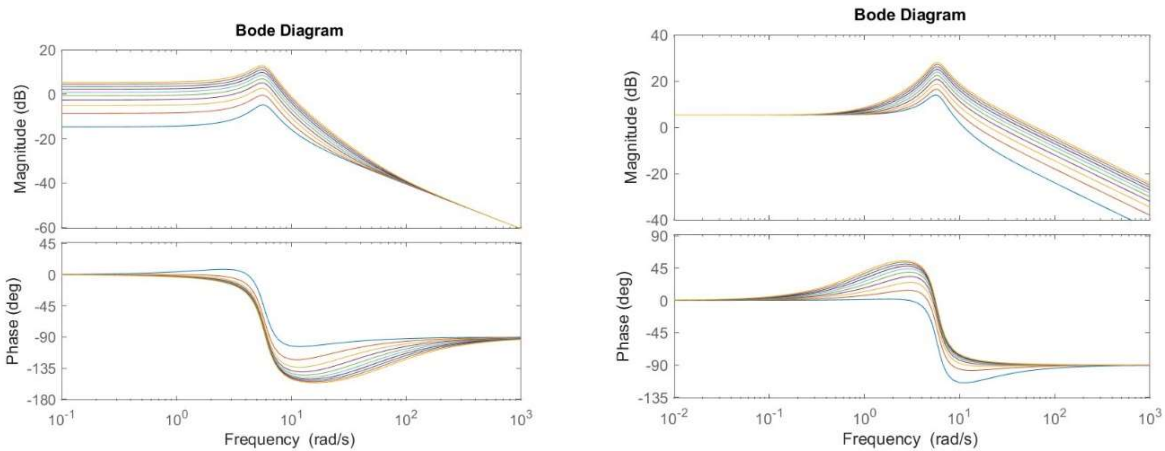


Figure 27: Bode diagram, fixed kd or kp (case 1)

In the first one, poles precede the zero; in the second one it's the opposite. In both cases, for whatever proportional and derivative gains, P_m is always positive, thus providing stability.

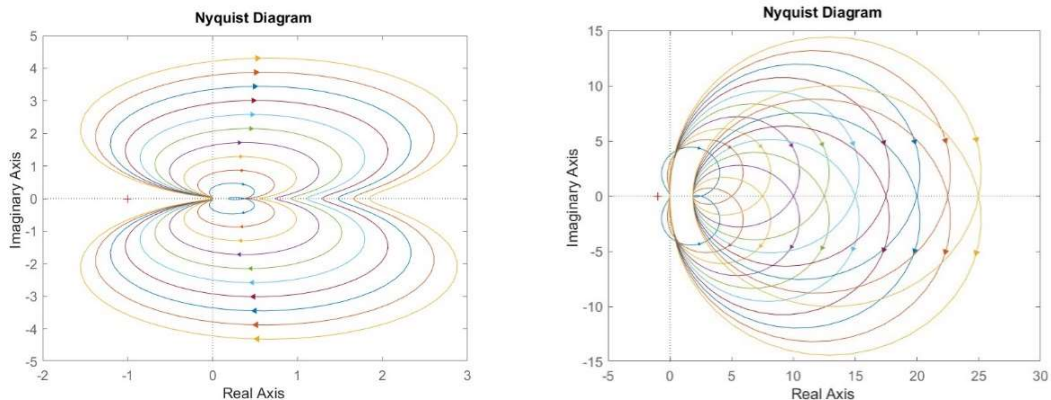


Figure 28: Nyquist diagram, fixed kd or kp (case 1)

Plotting instead the root locus (which varies at the same time, proportionally, k_P and k_D), we get no poles on the right side of the plane:

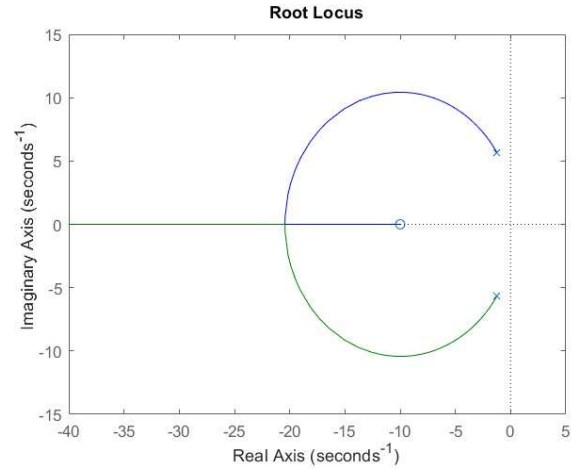


Figure 29: root locus - PD (case 1)

$$2) k_2 = 14.715 \text{ N/m.}$$

Performances:

i. Steady-state error (e_∞):

$$e_\infty = 0$$

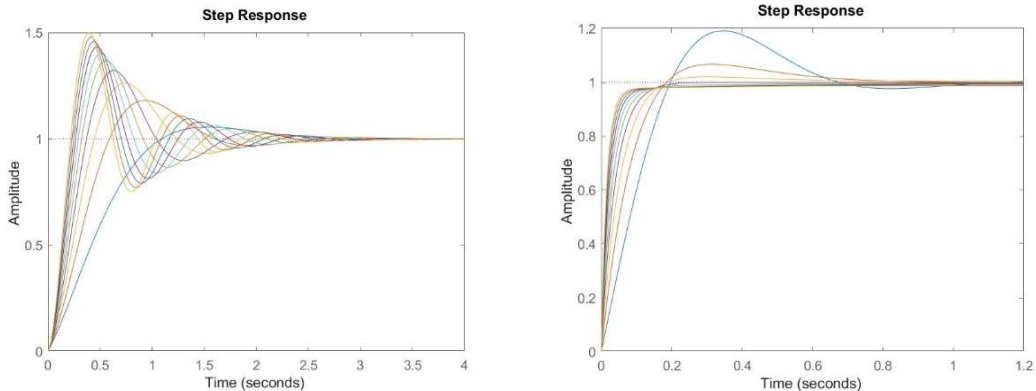


Figure 30: step response (case 2)

ii. Percentage overshoot (P.O.):

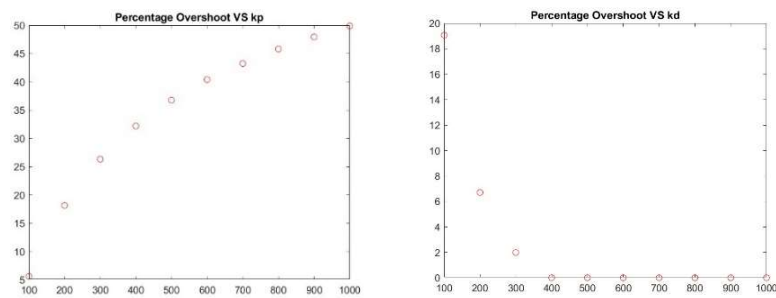


Figure 31: overshoot (case 2)

iii. Rise time (t_r):

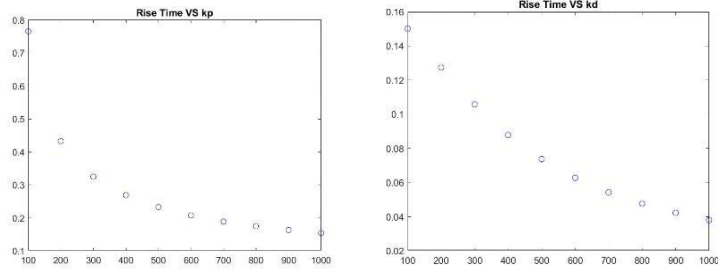


Figure 32: rise time (case 2)

iv. Settling time (t_s):

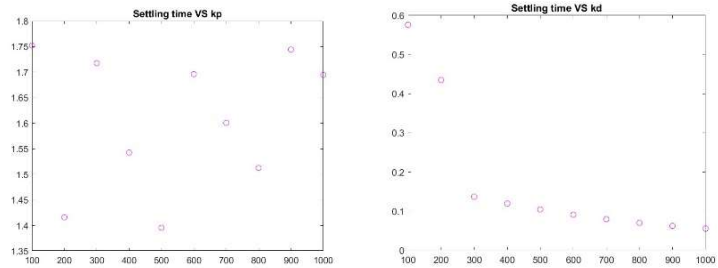


Figure 33: settling time (case 2)

For what concerns stability, Bode criterion can be applied: in all cases we get that the system is always stable. In the first case poles precede the only zero (and poles differ, being one negative and the other null); in the second one the zero precedes the only non-null pole instead (but they are quite close, as we can see in the phase that never gets above -60°). However, the second graph highlights both cases.

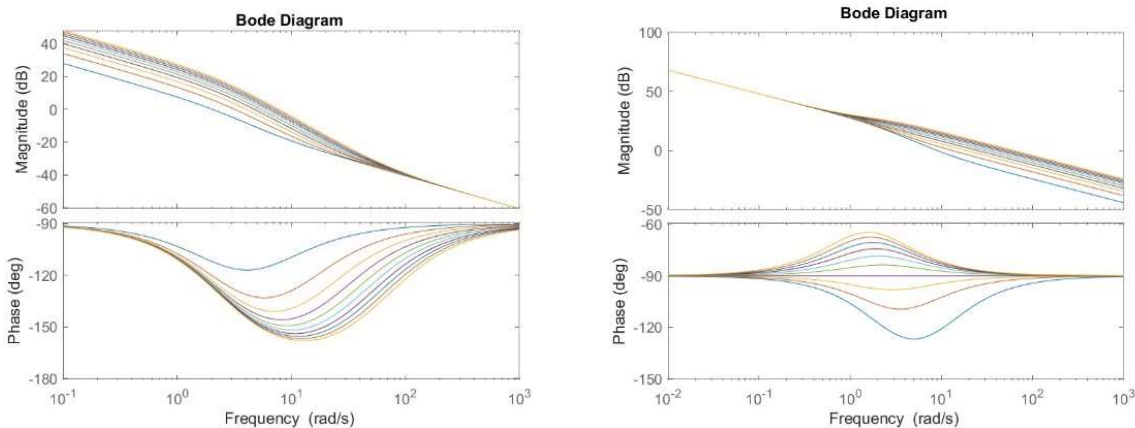


Figure 34: Bode diagram (case 2)

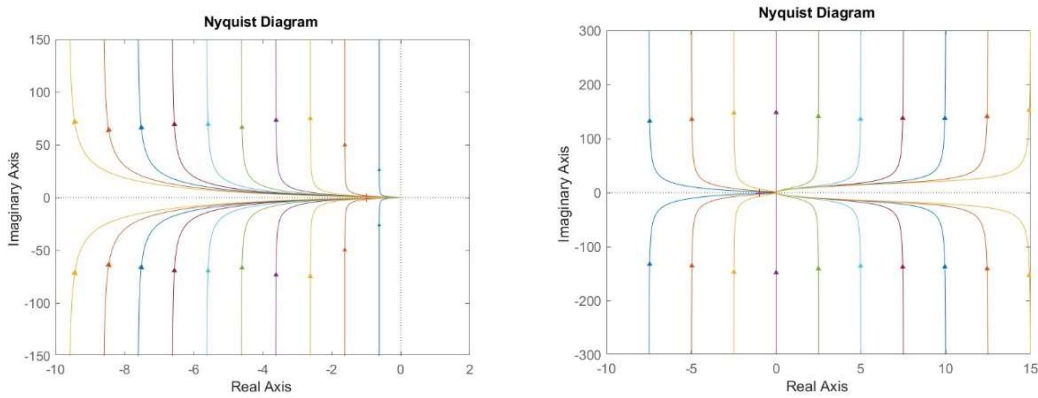


Figure 35: Nyquist diagram (case 2)

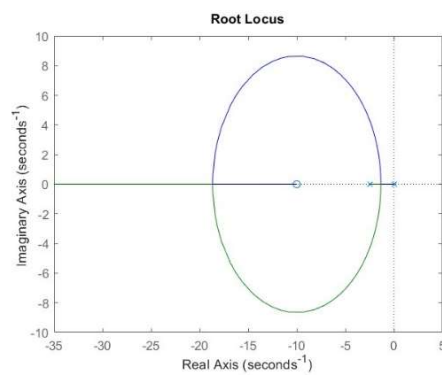


Figure 36: root locus (case 2)

3) $k_3 = 13 \text{ N/m}$.

Performances:

i. Steady-state error (e_∞):

$$e_\infty = \theta_{ref} - \theta_\infty = \theta_{ref} - \theta_{ref} \cdot \frac{k_p}{k^* + k_p} < 0$$

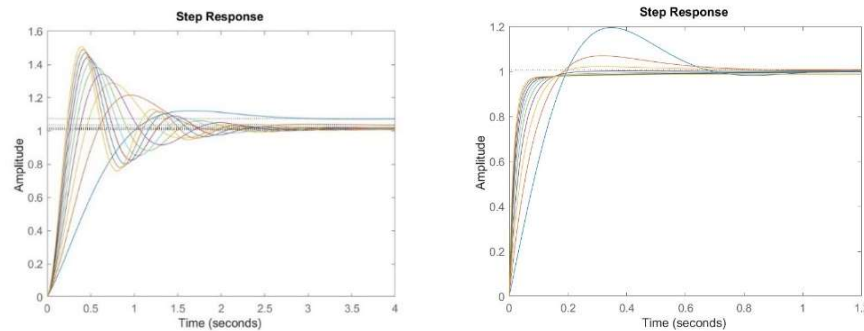


Figure 37: step response (case 3)

Response is above the reference due to a negative k^* .

ii. Percentage overshoot (P.O.):

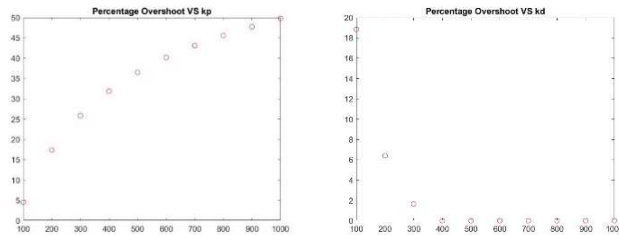


Figure 38: overshoot (case 3)

iii. Rise time (t_r):

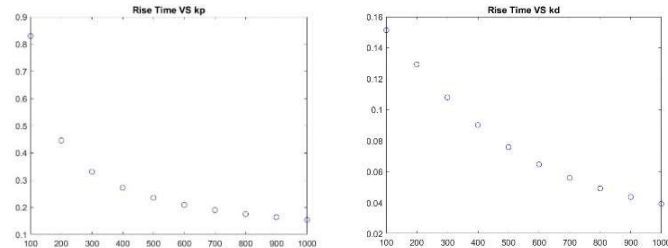


Figure 39: rise time (case 3)

iv. Settling time (t_s):

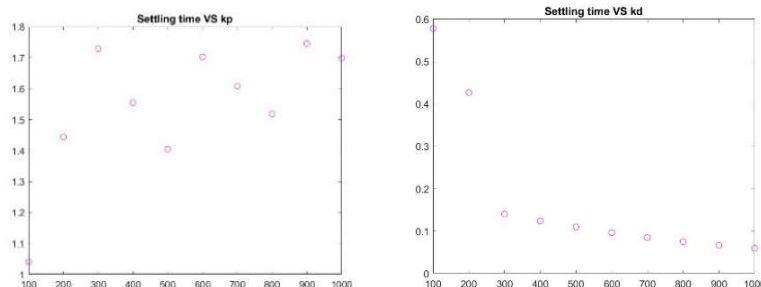


Figure 40: settling time (case 3)

For what concerns stability, Bode criterion cannot be applied (one unstable pole). Gain is negative; thus, phase is -180° at the beginning. Being there two poles (one positive and one negative), in the first case the zero is at the end (slope increases), while positive pole is at the beginning (phase increases). In the second graph we see both cases: pole(+), zero, pole(+) in the *upper* part and pole(+), pole(−), zero in the *lower*.

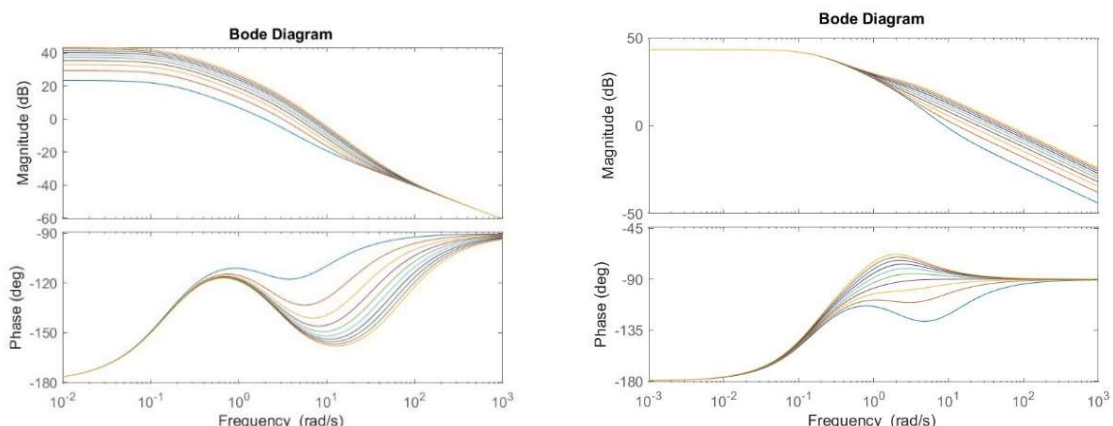


Figure 41: Bode diagram (case 3)

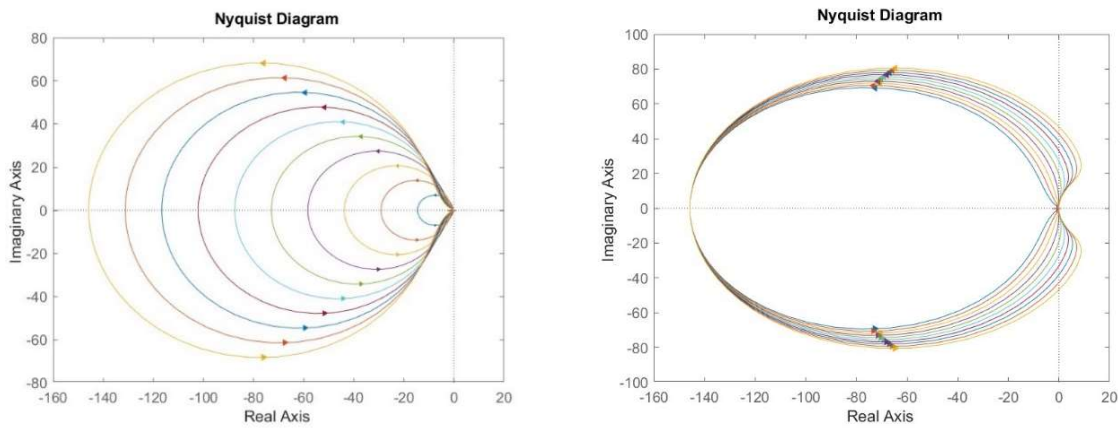


Figure 42: Nyquist diagram (case 3)

Only k_P enhances stability, making the system stable, while k_D has no effect on stability (Nyquist diagram changes slightly). This means that if we decrease k_P , we get to a point where the system is unstable (as we can see from the following root locus).

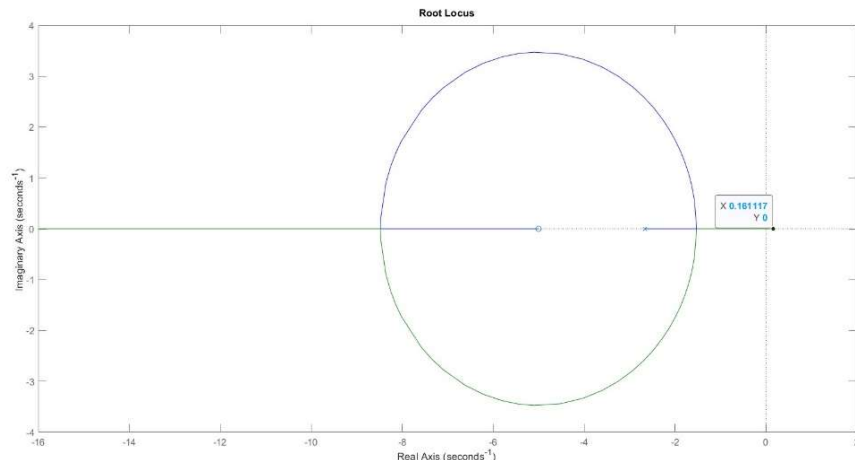


Figure 43: root locus (case 3)

1.3. Proportional and integral control (PI)

Equation of the controlled system is:

$$\begin{aligned}
 m^* \cdot \ddot{\theta} + c^* \cdot \dot{\theta} + k^* \cdot \theta &= C = k_P \cdot (\vartheta_{ref} - \vartheta) + k_I \cdot \int_0^t (\vartheta_{ref} - \vartheta) du \\
 y &= \int_0^t \vartheta du, \quad y_{ref} = \int_0^t \vartheta_{ref} du \Rightarrow \dot{y} = \vartheta, \quad \dot{y}_{ref} = \vartheta_{ref} \\
 m^* \cdot \ddot{y} + c^* \cdot \dot{y} + (k^* + k_P) \cdot \dot{y} + k_I \cdot y &= k_P \cdot \dot{y}_{ref} + k_I \cdot y_{ref}
 \end{aligned}$$

In the state-space form:

$$\begin{cases} m^* \cdot \ddot{y} + c^* \cdot \dot{y} + (k^* + k_p) \cdot \dot{y} + k_i \cdot y = k_p \cdot \dot{y}_{ref} + k_i \cdot y_{ref} \\ \ddot{y} = \ddot{y} \\ \dot{y} = \dot{y} \end{cases}$$

$$\begin{bmatrix} m^* & 0 & 0 \\ 0 & 1 & 0 \\ 0 & 0 & 1 \end{bmatrix} \cdot \begin{pmatrix} \ddot{y} \\ \dot{y} \\ y \end{pmatrix} + \begin{bmatrix} c^* & k^* + k_p & k_i \\ -1 & 0 & 0 \\ 0 & -1 & 0 \end{bmatrix} \cdot \begin{pmatrix} \ddot{y} \\ \dot{y} \\ y \end{pmatrix} = \begin{bmatrix} k_p & k_i \\ 0 & 0 \\ 0 & 0 \end{bmatrix} \cdot \begin{pmatrix} \dot{y}_{ref} \\ y_{ref} \end{pmatrix}$$

$$P = \begin{bmatrix} m^* & 0 & 0 \\ 0 & 1 & 0 \\ 0 & 0 & 1 \end{bmatrix}, \quad Q = \begin{bmatrix} c^* & k^* + k_p & k_i \\ -1 & 0 & 0 \\ 0 & -1 & 0 \end{bmatrix};$$

$$N = \begin{bmatrix} k_p & k_i \\ 0 & 0 \\ 0 & 0 \end{bmatrix}, \quad \underline{y} = \begin{pmatrix} \ddot{y} \\ \dot{y} \\ y \end{pmatrix}, \quad \underline{y}_{ref} = \begin{pmatrix} \dot{y}_{ref} \\ y_{ref} \end{pmatrix}.$$

$$A = -P^{-1} \cdot Q, \quad B = P^{-1} \cdot N.$$

Thus, we get: $\dot{y} = A \cdot \underline{y} + B \cdot \underline{y}_{ref}$: poles are the eigenvalues of A.

In Laplace domain, transfer functions (needed to apply the Final Value Theorem) are:

$$GH(s) = \frac{k_I + k_p \cdot s}{s \cdot (m^* \cdot s^2 + c^* \cdot s + k^*)} \Rightarrow L(s) = \frac{k_I + k_p \cdot s}{m^* \cdot s^3 + (c^* + k_D) \cdot s^2 + (k^* + k_p) \cdot s + k_I}$$

1) $k_1 = 150 \text{ N/m}$.

We vary k_D and k_I separately, with $k_p = 100:100:1000$ (while $k_I = 10$) and then $k_I = [10:10:50, 1800, 2000]$ for reasons that will be clarified following (while $k_p = 100$). Resulting performances:

i. Steady-state error (e_∞):

Final Value Theorem:

$$\theta_\infty = \lim_{t \rightarrow \infty} \theta(t) = \lim_{s \rightarrow 0} s \cdot \theta(s) = \lim_{s \rightarrow 0} s \cdot L(s) \cdot \theta_{ref} = \lim_{s \rightarrow 0} s \cdot L(s) \cdot \bar{\theta}_{ref}/s = \bar{\theta}_{ref}$$

$$\Rightarrow e_\infty = 0$$

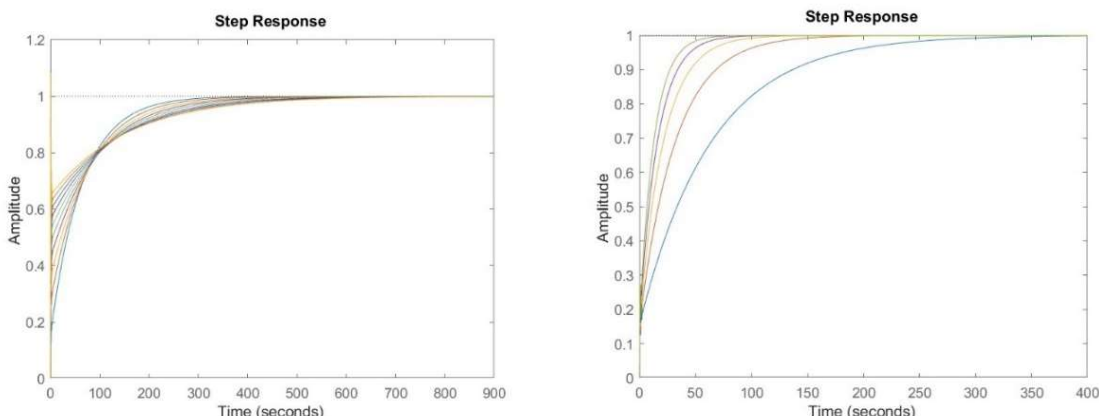


Figure 44: step response, fixed k_I and k_p (case 1)

Numerical results are coherent with theoretical ones. In the second graph only the stable systems' responses are plotted (in particular, the ones having k_I very high are unstable). Let's zoom on the beginning (III order system):

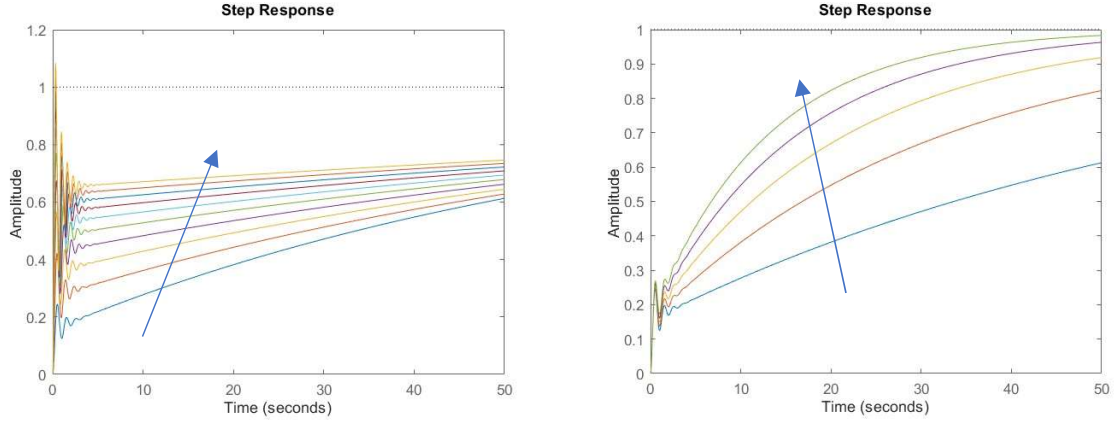


Figure 45: zoom on step response (case 1)

Oscillatory behavior is quickly replaced by a non-harmonic one.

No overshoot occurs (except for high values of k_P), so we can compute it only for very few cases in this simulation (thus we don't plot it).

ii. Rise time (t_r):

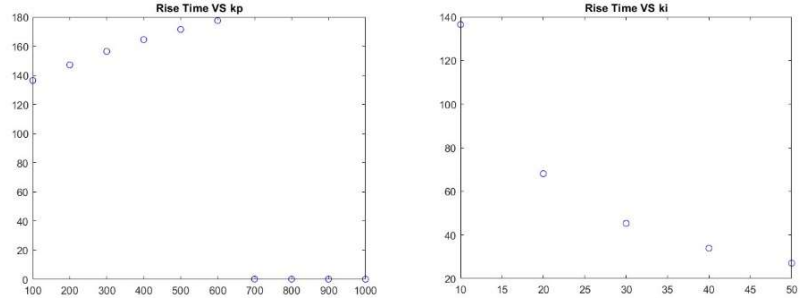


Figure 46: rise time, fixed ki and kp (case 1)

Rise time increases with k_P , only to decrease abruptly from a certain value on (in the graph it's not visible due to the scale, but if we zoom in it keeps decreasing). On the other hand, it decreases while k_I increases.

iii. Settling time (t_s):

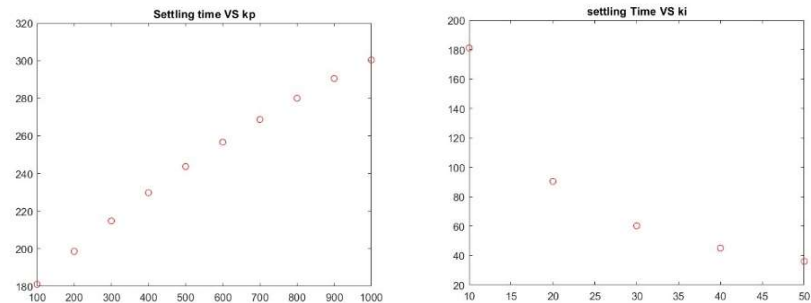


Figure 47: settling time, fixed ki and kp (case 1)

k_P tends to increase t_s here, while k_I does the opposite (obviously it has been computed only for stable cases).

If we look at the Bode diagram (criterion can be applied):

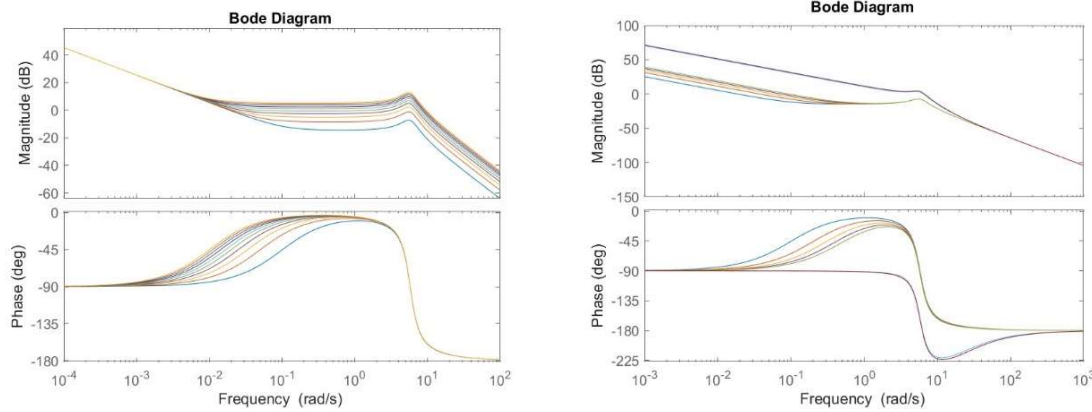


Figure 48: Bode diagram (case 1)

In the first diagram system is always stable, since P_m is never negative for all those combinations of gains: poles precede the zero in this case. In the second diagram, if we increase the value of k_1 (1800 and 2000) phase margin happens to be negative due to poles placed before the only zero: system becomes unstable. This occurs only for some combinations of parameters.

Same conclusion with Nyquist:

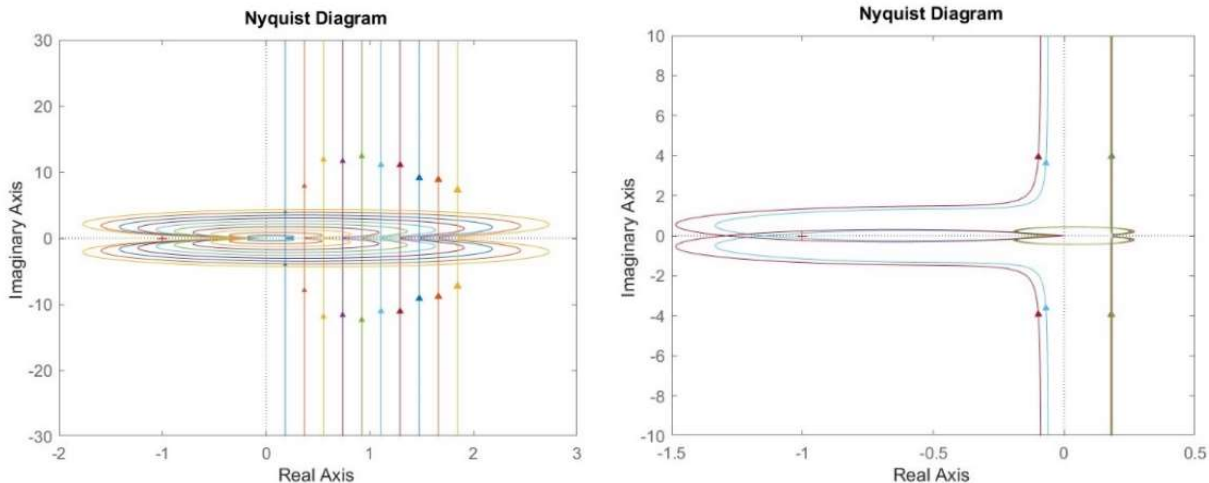


Figure 49: Nyquist diagram (case 1)

While in the first diagram no encirclements around $(-1; 0)$ occur, in the second one two diagrams (unstable ones) have two (clockwise) encirclements, meaning that these systems are unstable. Note that stable diagrams get close to the origin, then move away from it only to come back later (at -180°): this is due to the resonance.

Root locus highlights these two conditions of stability and instability (got by setting different $G(s)$ at the beginning):

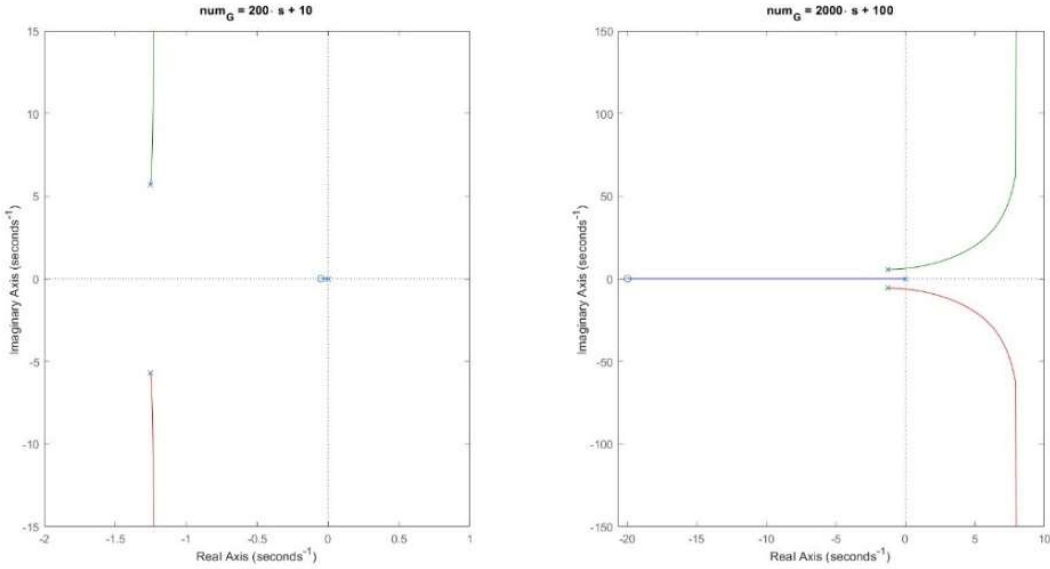


Figure 50: root locus, for 2 different conditions (case 1)

2) $k_2 = 14.715 \text{ N/m}$.

Performances:

i. Steady-state error (e_∞):

Due to the pole at the origin introduced by integral control, it is always null.

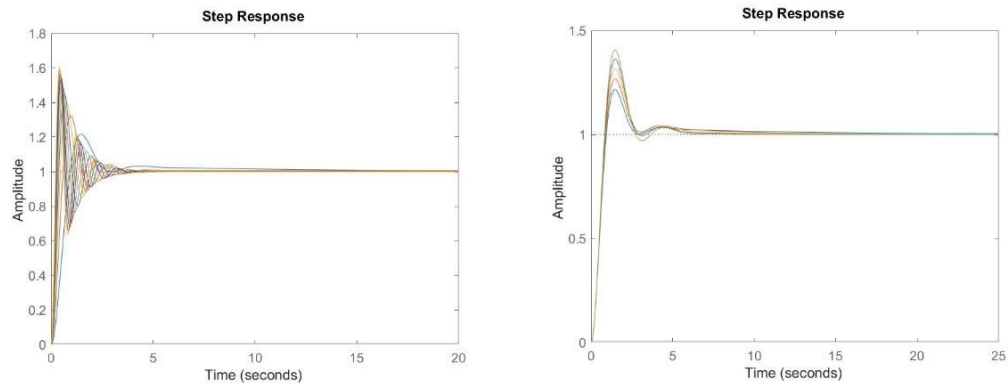


Figure 51: step response (case 2)

As before, we only plot stable steady-state responses.

ii. Percentage overshoot (P.O.):

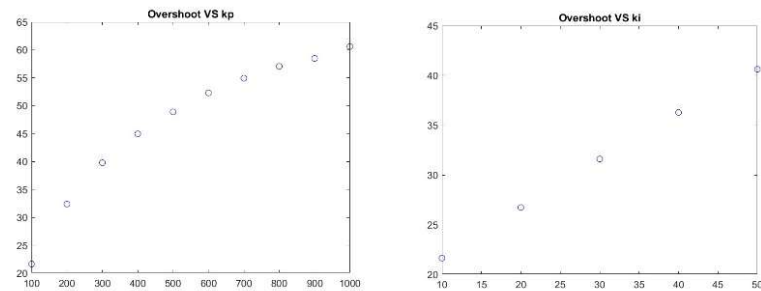


Figure 52: overshoot (case 2)

Increasing both margins P.O. increases accordingly.

iii. Rise time (t_r):

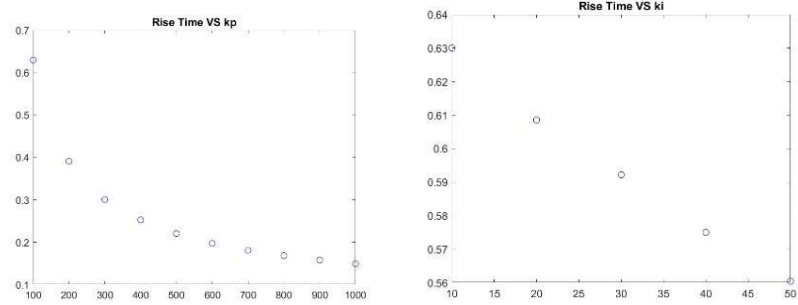


Figure 53: rise time (case 2)

Rise time is decreased by both margins.

iv. Settling time (t_s):

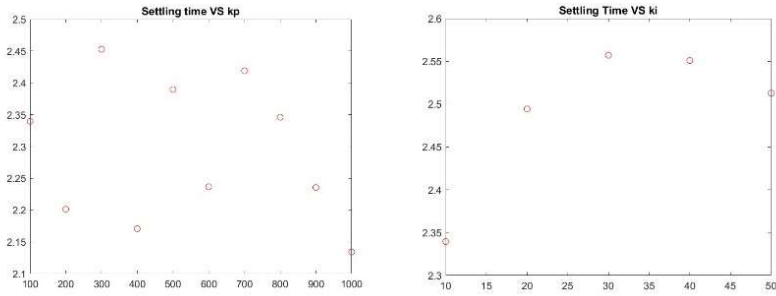


Figure 54: settling time (case 2)

k_p has no effect on t_s , while k_i decreases it after a certain threshold (and it increases it before).

Let's analyze stability ($k^* = 0$). System's minimum phase, so we apply Bode criterion. In the first graph the zero precedes the only non-null pole; for high k_i instead, the zero follows it (having a phase which gets lower than -180°). This will lead to instability.

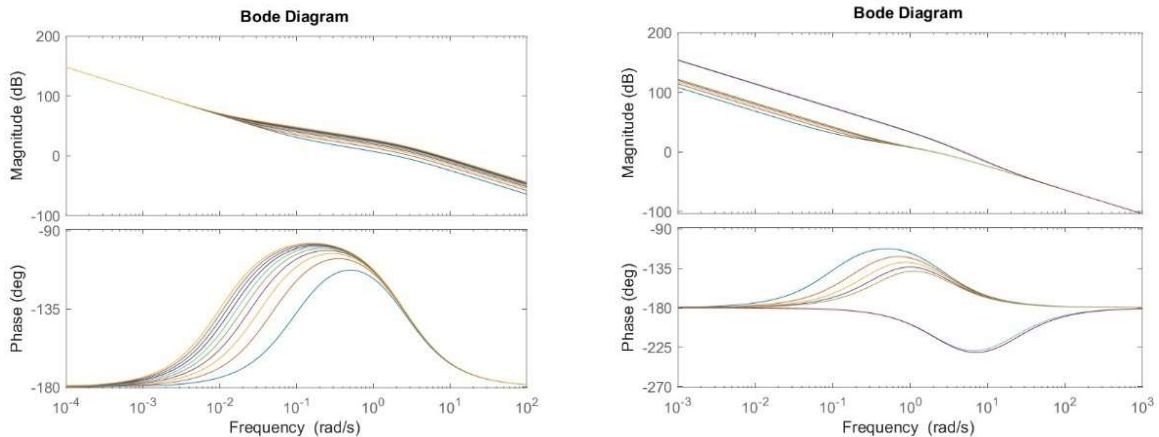


Figure 55: Bode diagram (case 2)

Two systems (the same as in case 1) are unstable, having negative phase margin. The same can be studied with the Nyquist criterion:

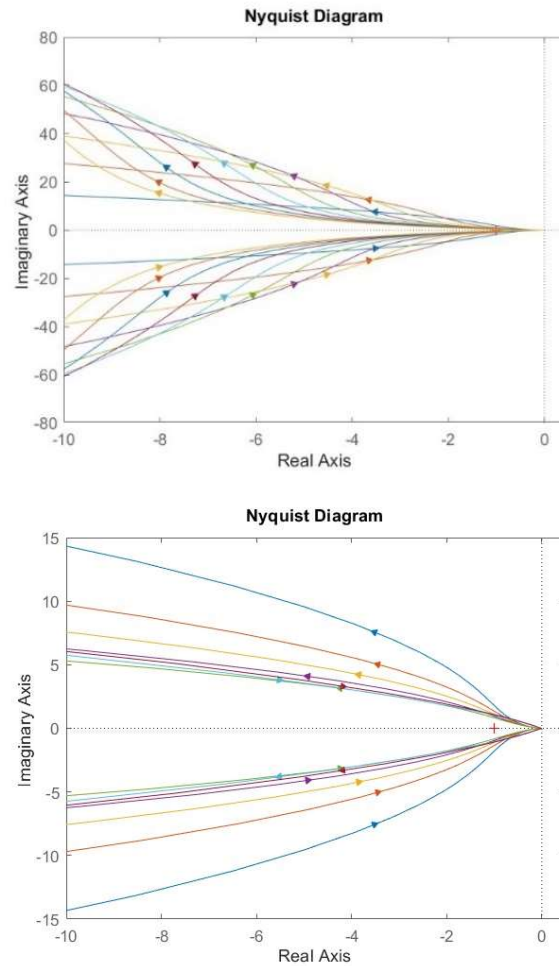


Figure 56: Nyquist diagram (case 2)

In all cases, due to two poles at the origin and to the initial phase equal to $-\pi$, diagrams all start from $(-\infty; 0)$ when $s \rightarrow 0$. However, remember that for $\Omega \in [0^+; +\infty]$ arrows are incoming in the origin; this means that stable ones have no encirclements around the origin, while unstable ones have two (clockwise) starting from an infinite location. This is the effect of having a double pole at the origin, one due to the integral control and the other due to $k^* = 0$.

As in precedence, unstable systems have the zero following the poles in Bode diagram.

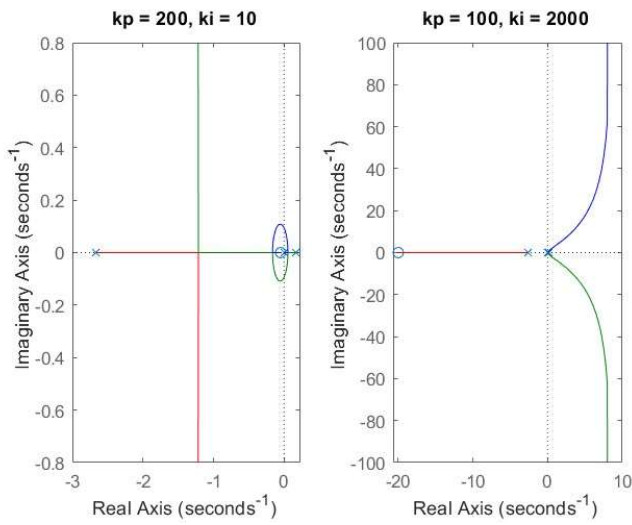


Figure 57: root locus (case 2)

3) $k_3 = 13 \text{ N/m}$.

Performances:

i. Steady-state error (e_∞):

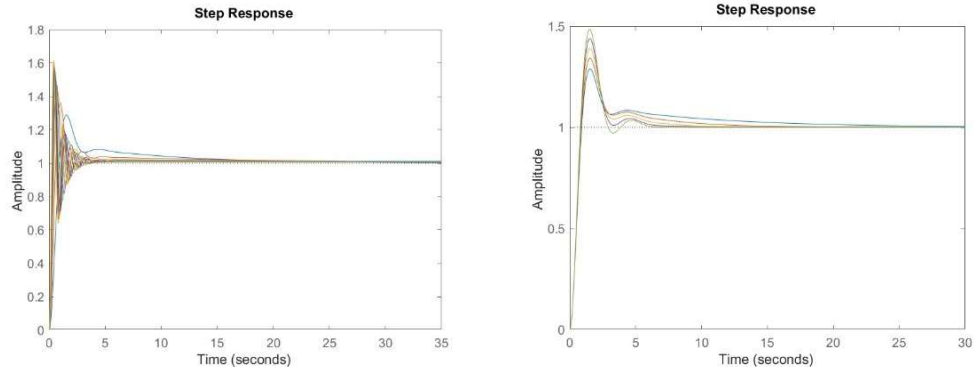


Figure 58: step response (case 3)

ii. Percentage overshoot (P.O.):

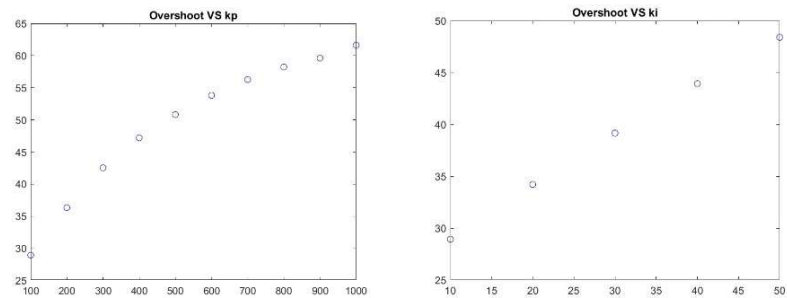


Figure 59: overshoot (case 3)

iii. Rise time (t_r):

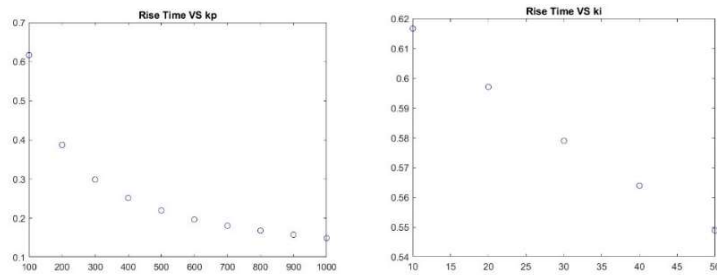


Figure 60: rise time (case 3)

iv. Settling time (t_s):

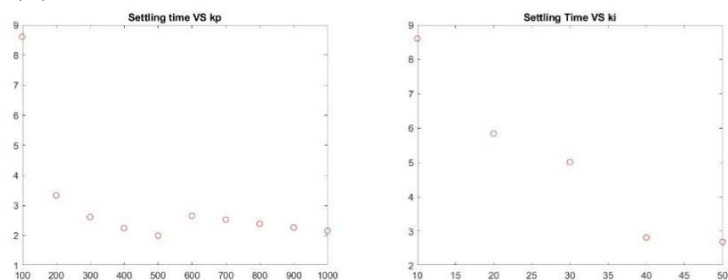


Figure 61: settling time (case 3)

Stability cannot be analyzed with Bode, since uncontrolled system is unstable.

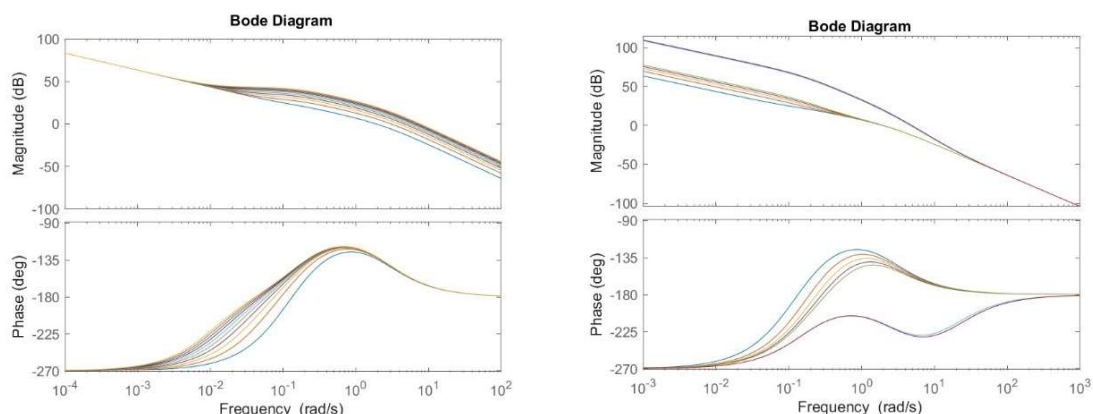


Figure 62: Bode diagram (case 3)

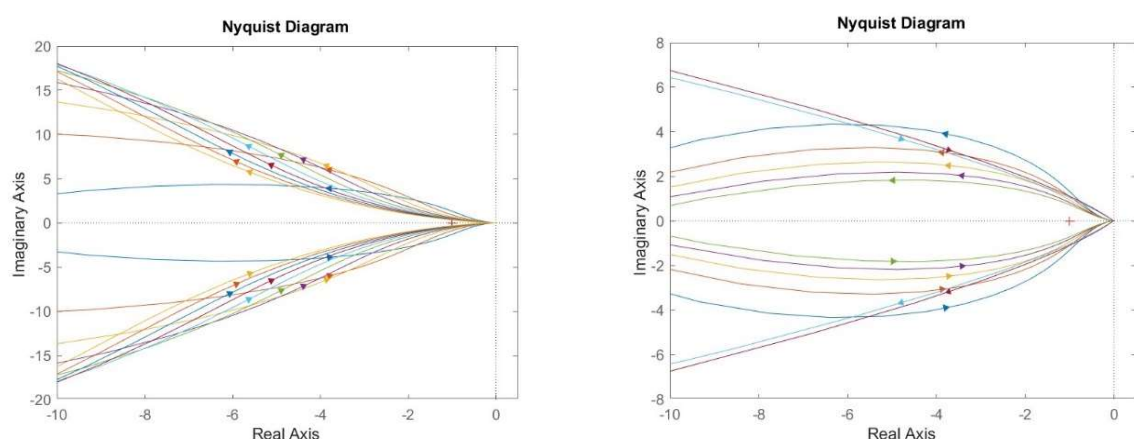


Figure 63: Nyquist diagram (case 3)

Gain is here negative, due to $k^* < 0$. Phase is -270° at the beginning because of this and of the pole at the origin. There are then two poles, respectively positive and negative (with the positive that always precedes the negative).

In the first graph, the sequence is: zero, poles (see how the slope behaves, becoming null at beginning and feeling the two following poles then). For high values of k_I the zero is at the end, leading to an unstable system. Moreover, system is unstable also for low values of k_P , with no encirclements around $(-1; 0)$ which come later.

Nyquist criterion is instead applicable: stable controlled systems show one counterclockwise encirclement around $(-1; 0)$; the two that are not stable have no encirclement, being their phase always higher than $-\pi$.

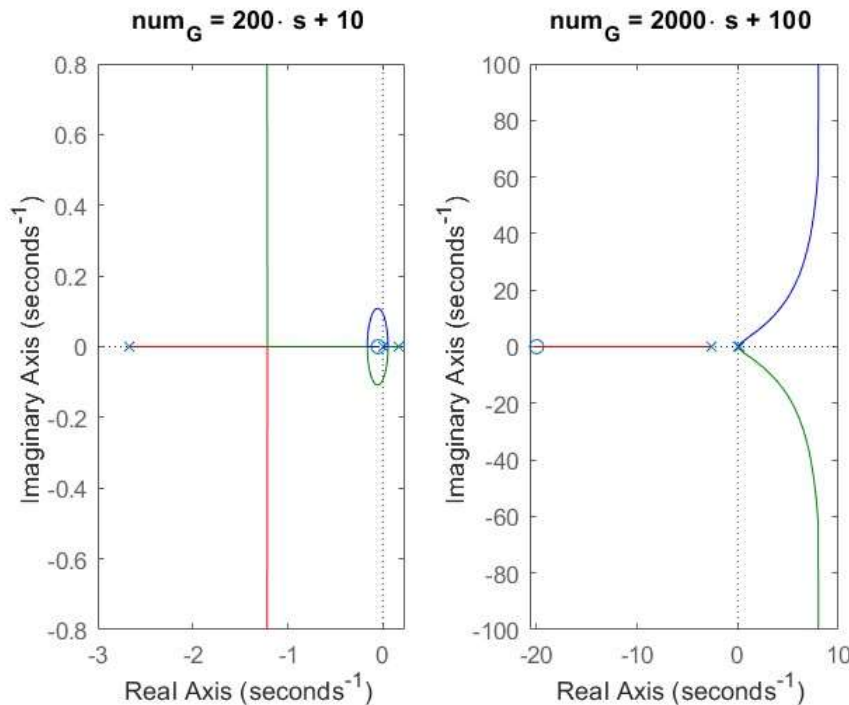


Figure 64: root locus (case 3)

In conclusion, system's unstable for (very) low values of k_P and for certain combinations of gain margins k_P and k_I .

2. Speed control of a rotor shaft

We focus on the mechanical system shown below:

$$C_m = C_m(\omega, y) \Rightarrow A = \frac{\partial C_m}{\partial \omega} \Big|_{\bar{\omega}, \bar{y}}, \quad B = \frac{\partial C_m}{\partial y} \Big|_{\bar{\omega}, \bar{y}}$$

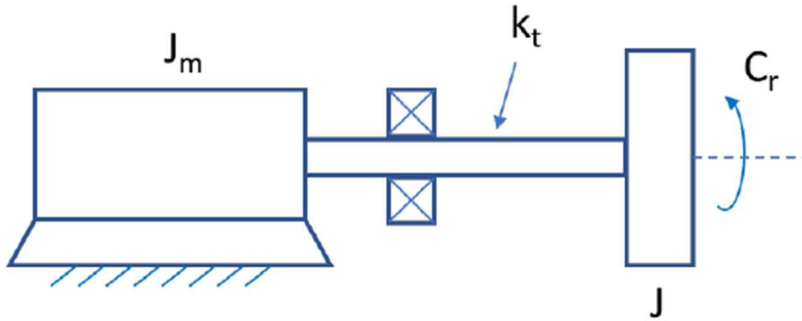


Figure 65: mechanical system

It represents an electric motor whose shaft is connected to an inertial load J and is subject to a constant resistance torque C_r . Flexibility of the shaft is taken into account through a torsional spring of constant k_t . Data are provided:

Table 3: system data

System data			
Motor mass moment of inertia	J_m	[kgm ²]	0.01
Rotor mass moment of inertia	J	[kgm ²]	0.15
Equivalent damping coefficient	c	[Nms/(rad/s)]	0.01
Derivative of characteristic curve with respect to the speed of motor shaft at steady state	A	[Nm/(rad/s)]	-0.986
Derivative of characteristic curve with respect to the control variable at steady state	B	[Nm/V]	1.1
Equivalent torsional spring	k_t	[Nm]	1000

2.1. CASE A: $k_t \rightarrow \infty$

In this case angular speed is constant along the shaft, and there's no potential energy in Lagrange energetical analysis:

$$\begin{aligned} E_c &= \frac{1}{2} \cdot (J_m + J) \cdot \omega^2 = \frac{1}{2} \cdot (J_m + J) \cdot \dot{\theta}^2 \\ D &= \frac{1}{2} \cdot c \cdot \omega^2 = \frac{1}{2} \cdot c \cdot \dot{\theta}^2 \\ \delta \mathcal{L} &= C_m \cdot \delta \vartheta - C_r \cdot \delta \vartheta \end{aligned}$$

The resulting differential equation is:

$$(J_m + J) \cdot \dot{\omega} + c \cdot \omega = C_m - C_r$$

Finding the steady-state condition and then linearizing (with $\delta\omega = \omega - \bar{\omega}$ and $\delta y = y - \bar{y}$):

$$(J_m + J) \cdot \delta\dot{\omega} + c \cdot \delta\omega + c \cdot \bar{\omega} = C_m(\bar{\omega}, \bar{y}) + A \cdot \delta\omega + B \cdot \delta y - C_r$$

Applying the steady-state condition:

$$c \cdot \bar{\omega} = C_m(\bar{\omega}, \bar{y}) - C_r$$

The linearized equation of motion becomes:

$$J^* \cdot \delta\dot{\omega} + (c - A) \cdot \delta\omega = B \cdot \delta y$$

Let's apply a proportional control to our system:

$$J^* \cdot \delta\dot{\omega} + (c - A + B \cdot k_p) \cdot \delta\omega = B \cdot k_p \cdot \delta\omega_{ref}$$

Uncontrolled system is stable; in fact, the only eigenvalue is:

$$\lambda = -\frac{c - A}{J^*} = -6.225 < 0$$

From time domain analysis, controlled system is always stable too ($\forall k_p$):

$$\lambda_c = -\frac{c - A + B \cdot k_p}{J^*} = \lambda - \frac{B \cdot k_p}{J^*} < \lambda < 0$$

Varying proportional gain in the interval 10:10:100, step response becomes:

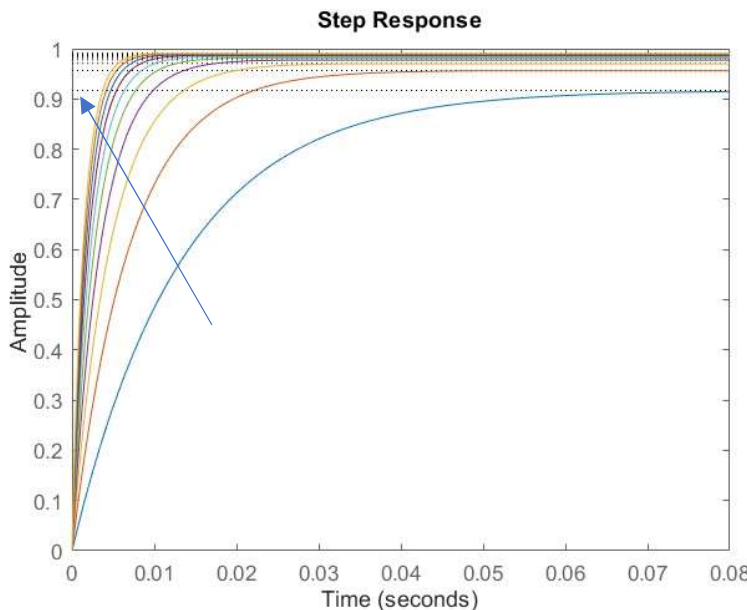


Figure 66: step response (rigid shaft)

Since first order systems don't oscillate, there is no overshoot.

Performances:

- i. Steady-state error (e_∞):

Solving the following differential equation ($t > 0$ and $\delta\omega(t = 0) = 0$):

$$J^* \cdot \delta\dot{\omega} + (c - A + B \cdot k_p) \cdot \delta\omega = B \cdot k_p \cdot \delta\bar{\omega}_{ref}$$

Response to step input is:

$$\delta\omega(t) = \frac{B \cdot k_p}{c - A + B \cdot k_p} \cdot \delta\bar{\omega}_{ref} \cdot [1 - e^{-t/\tau}] \Rightarrow e_{\infty} = \frac{c - A}{c - A + B \cdot k_p} \cdot \delta\bar{\omega}_{ref}$$

The higher k_p , the lower the steady-state error.

ii. Rise time (t_r):

It decreases according to an increase of k_p .

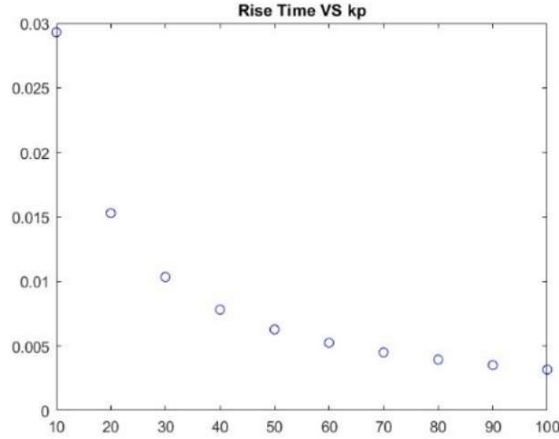


Figure 67: rise time (rigid shaft)

iii. Settling time (t_s):

It decreases if k_p increases, due to a more “horizontal” approaching of the curves to their asymptotes.

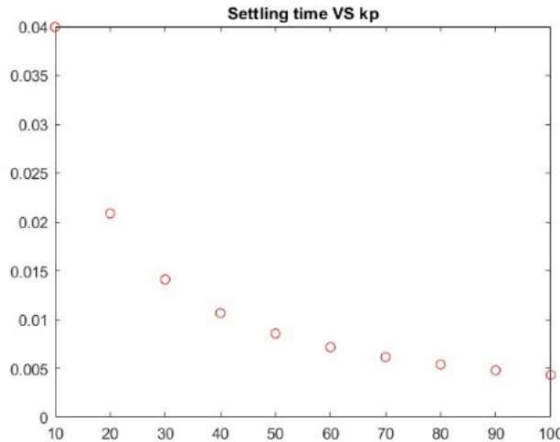


Figure 68: settling time (rigid shaft)

Let's analyze now stability of the system in Laplace domain; as said, from time domain's analysis we found system's always stable too.

$$GH(s) = \frac{k_p \cdot B}{J^* \cdot s + (c - A)} \Rightarrow L(s) = \frac{k_p \cdot B}{J^* \cdot s + (c - A) + k_p \cdot B}$$

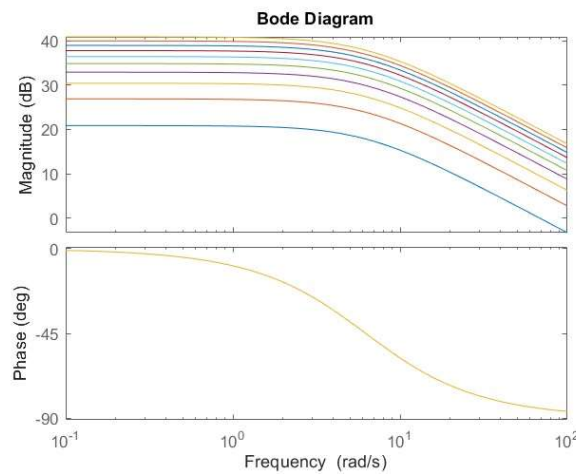


Figure 69: Bode diagram (rigid shaft)

System's minimum phase, so Bode criterion can be applied ($Pm > 0 \forall k_p$: stable).

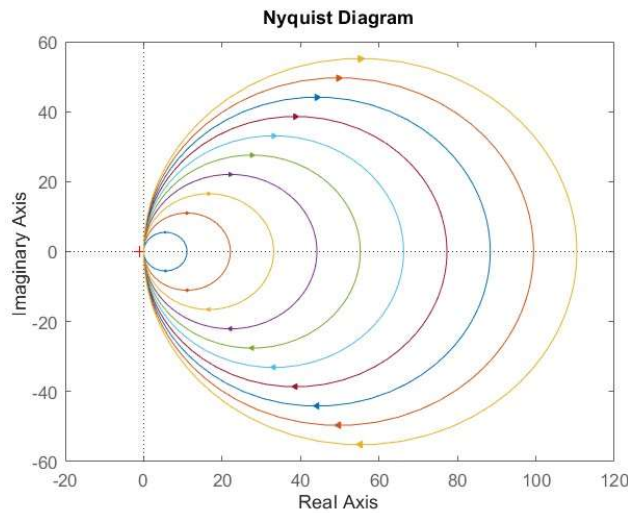


Figure 70: Nyquist diagram (rigid shaft)

No encirclement around $(-1; 0)$, as there are no unstable poles of the uncontrolled system: stable.

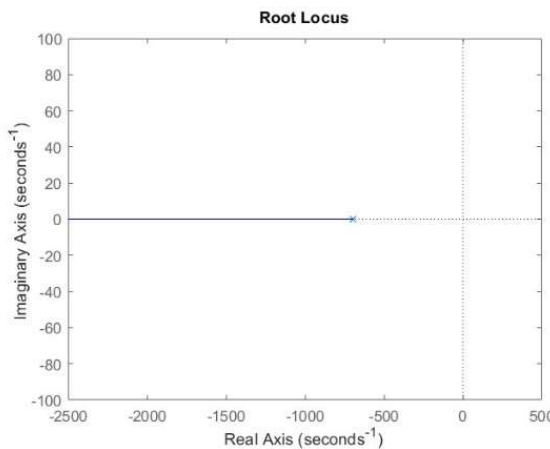


Figure 71: root locus (rigid shaft)

All poles are negative real values (providing non-oscillatory behavior); thus, stability is assured.

2.2. CASE B: shaft flexibility (torsional spring k_t)

When k_p is increased, system becomes faster (and the bandwidth gets wider); it cannot be considered rigid anymore, so the idea of flexible shaft is introduced. Let's name the motor angular speed ω_1 (angle θ_1) and the rotor one ω_2 (angle θ_2). This way we introduce a potential energy term:

$$\begin{aligned} E_c &= \frac{1}{2} \cdot J_m \cdot \omega_1^2 + \frac{1}{2} \cdot J \cdot \omega_2^2 = \frac{1}{2} \cdot J_m \cdot \dot{\theta}_1^2 + \frac{1}{2} \cdot J \cdot \dot{\theta}_2^2 \\ D &= \frac{1}{2} \cdot c \cdot \omega_1^2 + \frac{1}{2} \cdot c \cdot \omega_2^2 \\ V &= \frac{1}{2} \cdot k_T \cdot (\theta_1 - \theta_2)^2 \\ \delta\mathcal{L} &= C_m \cdot \delta\vartheta_1 - C_r \cdot \delta\vartheta_2 \end{aligned}$$

The resulting differential equations are:

$$\begin{cases} J_m \cdot \ddot{\theta}_1 + c \cdot \dot{\theta}_1 + k_T \cdot (\theta_1 - \theta_2) = C_m \\ J_m \cdot \ddot{\theta}_2 + c \cdot \dot{\theta}_2 + k_T \cdot (\theta_2 - \theta_1) = -C_r \end{cases}$$

Let's compute the position around which variables deviate; being the relative angle $\theta_{rel} = \theta_1 - \theta_2$ constant in steady-state condition, and $\omega_1 = \omega_2 = \bar{\omega}$:

$$\begin{cases} c \cdot \bar{\omega} + k_T \cdot \bar{\theta}_{rel} = C_m(\bar{\omega}, \bar{y}) \\ c \cdot \bar{\omega} - k_T \cdot \bar{\theta}_{rel} = -C_r \end{cases} \Rightarrow 2 \cdot c \cdot \bar{\omega} = C_m(\bar{\omega}, \bar{y}) - C_r$$

Fixing $\bar{\omega}$, we find \bar{y} ; $2 \cdot k_T \cdot \bar{\theta}_{rel} = C_m(\bar{\omega}, \bar{y})$, finding $\bar{\theta}_{rel}$.

Linearizing the system and exploiting the steady-state condition:

$$\begin{cases} J_m \cdot \delta\ddot{\theta}_1 + c \cdot (\bar{\omega} + \delta\dot{\theta}_1) + k_T \cdot (\delta\theta_{rel} + \bar{\theta}_{rel}) = C_m(\bar{\omega}, \bar{y}) + A \cdot \delta\dot{\theta}_1 + B \cdot \delta y \\ J_m \cdot \delta\ddot{\theta}_2 + c \cdot (\bar{\omega} + \delta\dot{\theta}_2) - k_T \cdot (\delta\theta_{rel} + \bar{\theta}_{rel}) = -C_r \end{cases}$$

$$\begin{cases} J_m \cdot \delta\ddot{\theta}_1 + c \cdot \delta\dot{\theta}_1 + k_T \cdot (\delta\theta_1 - \delta\theta_2) = A \cdot \delta\dot{\theta}_1 + B \cdot \delta y \\ J_m \cdot \delta\ddot{\theta}_2 + c \cdot \delta\dot{\theta}_2 + k_T \cdot (\delta\theta_2 - \delta\theta_1) = 0 \end{cases}$$

$$\begin{bmatrix} J_m & 0 \\ 0 & J \end{bmatrix} \cdot \begin{pmatrix} \delta\ddot{\theta}_1 \\ \delta\ddot{\theta}_2 \end{pmatrix} + \begin{bmatrix} c & A \\ 0 & c \end{bmatrix} \cdot \begin{pmatrix} \delta\dot{\theta}_1 \\ \delta\dot{\theta}_2 \end{pmatrix} + \begin{bmatrix} k_T & -k_T \\ -k_T & k_T \end{bmatrix} \cdot \begin{pmatrix} \delta\theta_1 \\ \delta\theta_2 \end{pmatrix} = \begin{bmatrix} B \\ 0 \end{bmatrix} \cdot \delta y$$

Let's analyze stability in Laplace domain. Systems are minimum phase; in fact, if we consider:

$$\begin{bmatrix} J_m & 0 \\ 0 & J \end{bmatrix} \cdot \underline{\mathcal{Z}}(s) + \begin{bmatrix} c & A \\ 0 & c \end{bmatrix} \cdot \dot{\underline{\mathcal{Z}}}(s) + \begin{bmatrix} k_T & -k_T \\ -k_T & k_T \end{bmatrix} \cdot \underline{\mathcal{Z}}(s) = \underline{\mathcal{C}} \Rightarrow \underline{\mathcal{Z}}(s) = [D(s)] \cdot \underline{\mathcal{C}}(s)$$

$$[D(s)] = ([M] \cdot s^2 + [C] \cdot s + [K])^{-1}$$

However, we know that:

$$\underline{C}(s) = \begin{bmatrix} B \\ 0 \end{bmatrix} \cdot \delta Y(s)$$

$$\underline{Z}(s) = \begin{bmatrix} (J \cdot s^2 + c \cdot s + k_T) \cdot B \\ \frac{\det([D(s)])}{k_T \cdot B} \\ \frac{\det([D(s)])}{\det([D(s)])} \end{bmatrix} \cdot \delta Y(s)$$

$$\det([D(s)]) = ((J_m \cdot J \cdot s^3 + (J \cdot (c - A) + J_m \cdot c) \cdot s^2 + ((J_m + J) \cdot k_T + c \cdot (c - A)) \cdot s + (c \cdot k_T + (c - A) \cdot k_T)) \cdot s$$

Zeros of $\det([D(s)])$ all have negative real part, meaning absence of unstable poles of the uncontrolled system.

1) CO-LOCATED CONTROL.

y is a generic control variable, such as voltage in DC motors, we must control.

$$\delta y = k_p \cdot (\delta \dot{\theta}_{ref} - \delta \dot{\theta}_1)$$

From the feedback control analysis, we get (including the "s" to derive):

$$GH(s) = \frac{\delta \Omega_1}{\delta \Omega_{ref} - \delta \Omega_1} =$$

$$\frac{k_p \cdot B \cdot (J \cdot s^2 + c \cdot s + k_T)}{(J_m \cdot J \cdot s^3 + (J \cdot (c - A) + J_m \cdot c) \cdot s^2 + ((J_m + J) \cdot k_T + c \cdot (c - A)) \cdot s + (c \cdot k_T + (c - A) \cdot k_T)}$$

Consequently:

$$L(s) = \frac{\delta \Omega_1}{\delta \Omega_{ref}} =$$

$$\frac{k_p \cdot B \cdot (J \cdot s^2 + c \cdot s + k_T)}{(J_m \cdot J \cdot s^3 + (J \cdot (c - A) + J_m \cdot c + k_p \cdot B \cdot J) \cdot s^2 + ((J_m + J) \cdot k_T + c \cdot (c - A) + k_p \cdot B \cdot c) \cdot s + (c \cdot k_T + (c - A + k_p \cdot B) \cdot k_T)}$$

Varying proportional gain in 10:10:100, step response becomes (III order system):

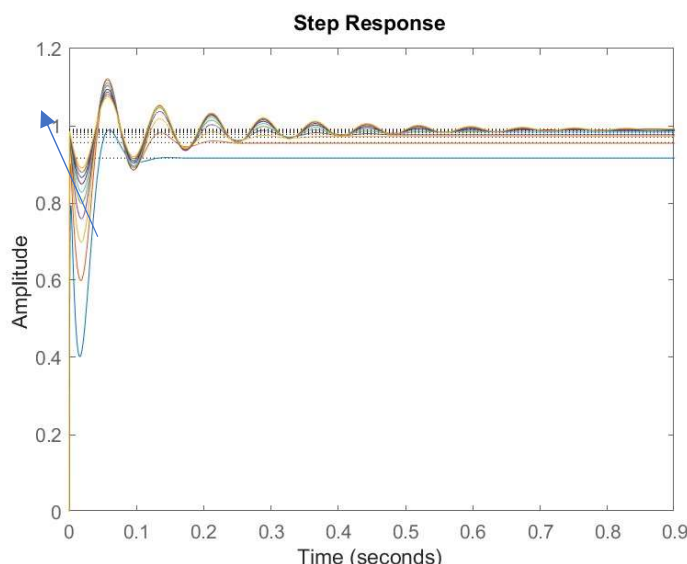


Figure 72: step response (collocated control)

Oscillatory behavior is visible (third order system): rise time is extremely small, as we can see analyzing performances:

i. Percentage overshoot (P.O.):

We can observe a non-monotonous trend.

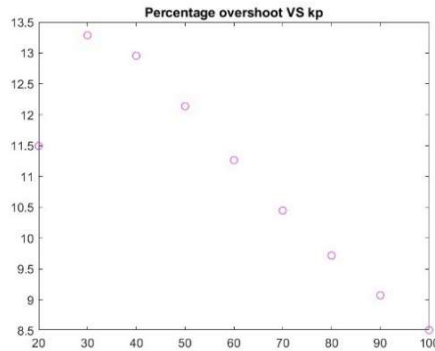


Figure 73: percentage overshoot (colocated control)

ii. Rise time (t_r):

As noticed, it is very low.

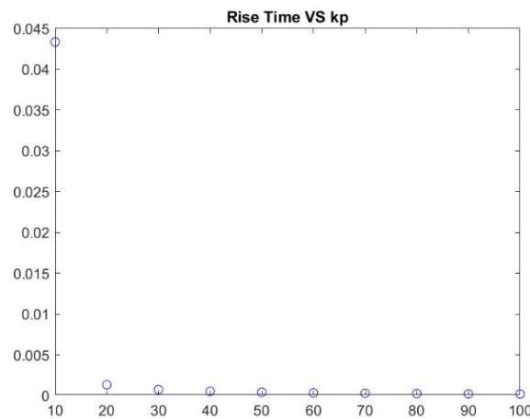


Figure 74: rise time (colocated control)

iii. Settling time (t_s):

It tends to stabilize.

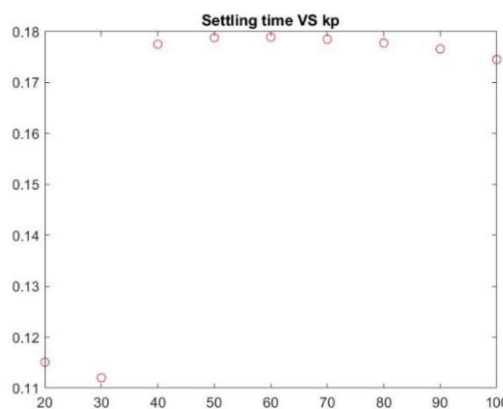


Figure 75: settling time (colocated control)

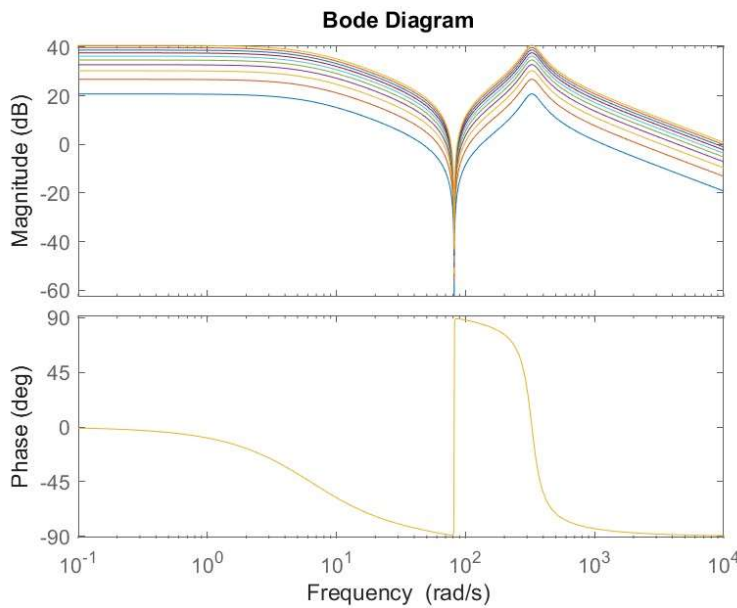


Figure 76: Bode diagram (collocated control)

We observe here the presence of antiresonance, due to two conjugate zeros; on the other hand, P_m is always positive, whatever value of k_p we choose.

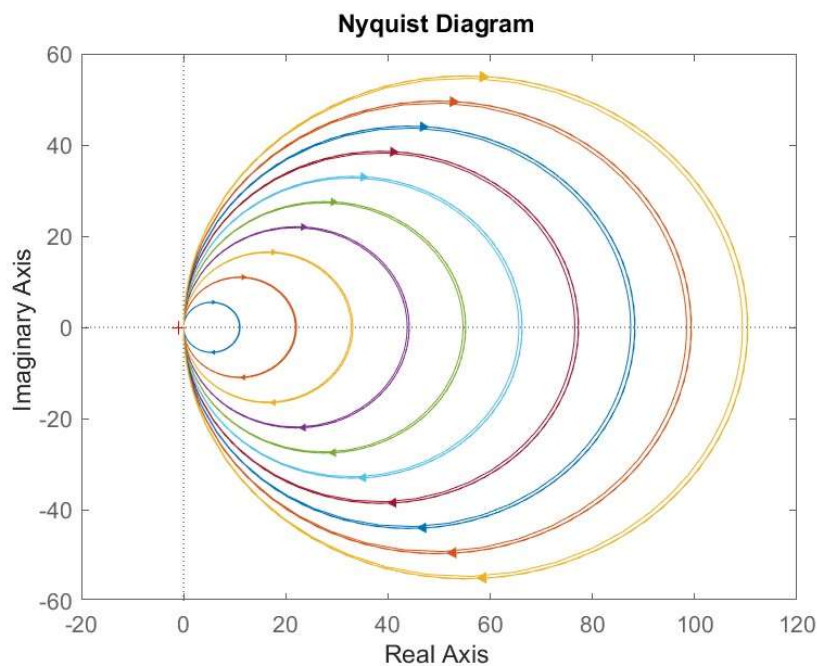


Figure 77: Nyquist diagram (collocated control)

Same conclusion with the Nyquist diagram and the Root locus too.

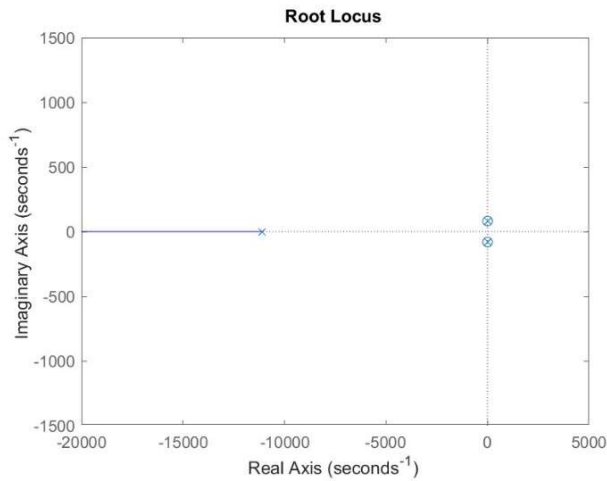


Figure 78: root locus (colocated control)

2) NON-CO-LOCATED CONTROL

$$\delta y = k_p \cdot (\delta \dot{\theta}_{ref} - \delta \dot{\theta}_2)$$

From the feedback control analysis, we get:

$$GH(s) = \frac{\delta \Omega_2}{\delta \Omega_{ref} - \delta \Omega_2} = \frac{k_p \cdot B \cdot k_T}{(J_m \cdot J \cdot s^3 + (J \cdot (c - A) + J_m \cdot c) \cdot s^2 + ((J_m + J) \cdot k_T + c \cdot (c - A)) \cdot s + (c \cdot k_T + (c - A) \cdot k_T)}$$

Consequently:

$$L(s) = \frac{\delta \Omega_2}{\delta \Omega_{ref}} = \frac{k_p \cdot B \cdot k_T}{(J_m \cdot J \cdot s^3 + (J \cdot (c - A) + J_m \cdot c) \cdot s^2 + ((J_m + J) \cdot k_T + c \cdot (c - A)) \cdot s + (c \cdot k_T + (c - A + k_p \cdot B) \cdot k_T)}$$

Varying proportional gain in 5:5:50, step response becomes (plotting only stable ones):

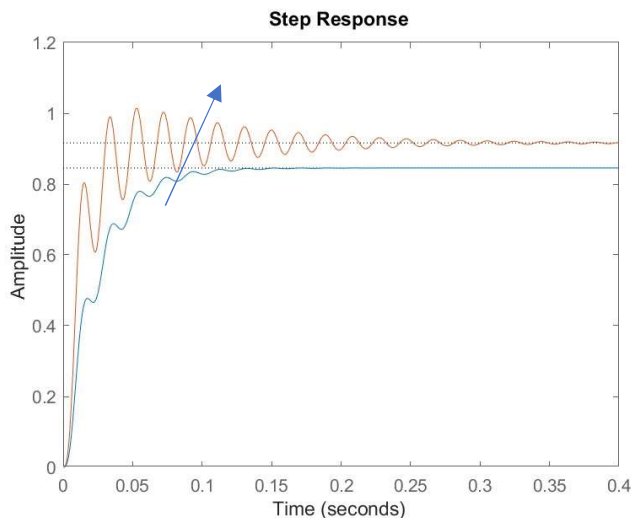


Figure 79: step response (non-colocated control)

If k_p increases, system quickly becomes unstable; performances have not been plotted due to this behavior for most values of k_p . In Laplace domain, Bode diagram is:

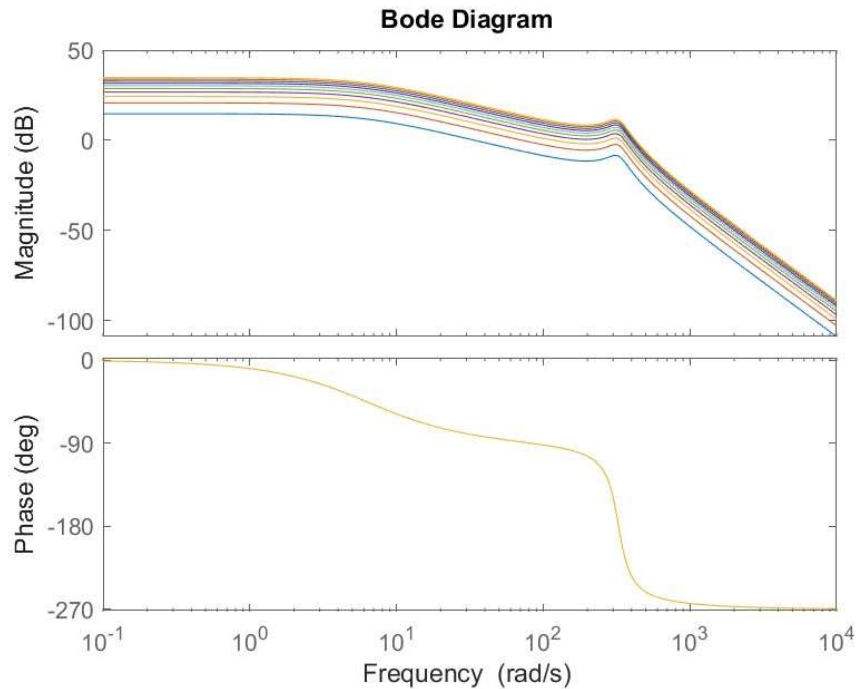


Figure 80: Bode diagram (non-collocated control)

For increasing values of k_p , phase margin becomes negative (and gain margin too). The same can be seen with Nyquist criterion: *two* clockwise encirclements result in an unstable controlled system.

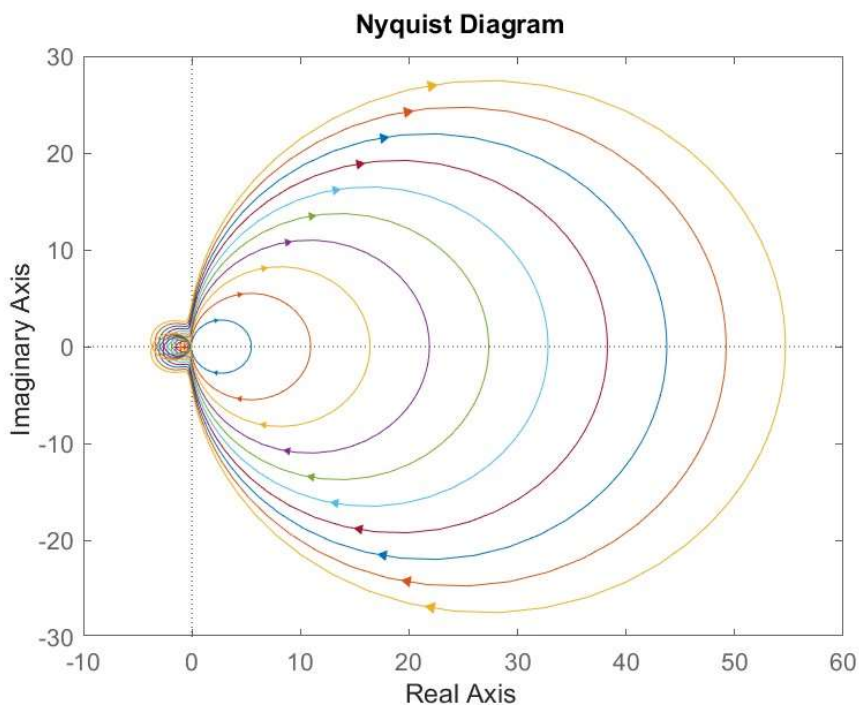


Figure 81: Nyquist diagram (non-collocated system)

Root locus of the system is instead:

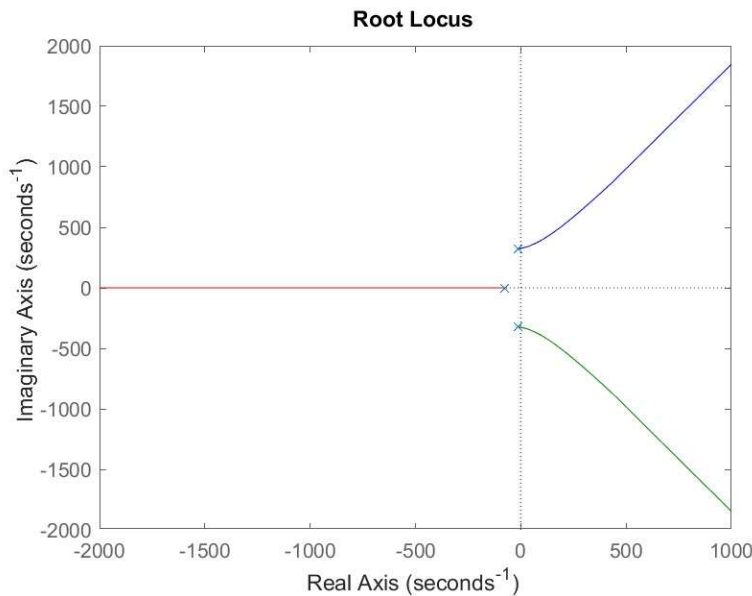


Figure 82: root locus (non-collocated control)

From a certain value of k_P on, controlled system has *two* unstable poles (as the number of encirclements around $(-1; 0)$). These poles are symmetric with respect to the real axis, having the same oscillation frequency: it's a typical case of *flutter instability*.

3. Control of trajectory of the workpiece of a machine tool

We focus on the machine tool shown below:

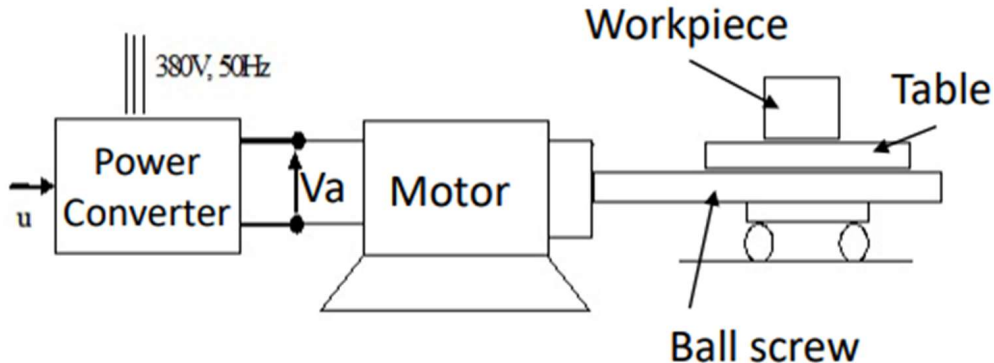


Figure 83: machine tool scheme

The shaft of an electric DC motor (inductance L_a , resistance R_a and motor constant $k\psi$) is connected to a ball screw (transmission ratio τ) that moves the table of the machine and the workpiece, which are fixed together. The shaft's flexibility is taken into account through a torsional spring of constant k_T , its damping through c_T . Workpiece must be moved of 1 m in 1.5 s following a 1/3, 1/3, 1/3 motion law in speed. Data are here provided:

Table 4: system data

System data			
Final displacement	h	[m]	1
Final time	t_f	[s]	1.5
Motor mass moment of inertia	J_m	[kgm ²]	0.005
Motor shaft torsional stiffness	k_T	[Nm/rad]	1000
Motor shaft torsional damping	c_T	[Nms/rad]	2
Motor resistance	R_a	[Ω]	1.2
Motor inductance	L_a	[H]	0.008
Motor constant	$k\psi$	[Vs/rad]	0.8
Ball screw ratio	τ	[m/rad]	0.1/(2*π)
Ball screw efficiency	η	[-]	1
Equivalent coefficient for energy dissipation	c_d	[Ns/m]	10
Machine table mass + workpiece mass	$m_t + m_p$	[kg]	40

Reference in acceleration will always be modelled through the superposition of four different step signals, with delayed step times and opposite signs. References in speed and displacement will be obtained then integrating the reference in acceleration.

3.1. CASE A: $L_a = 0, k_t \rightarrow \infty$.

We look for the equations of motion:

$$E_c = \frac{1}{2} \cdot J_m \cdot \omega^2 + \frac{1}{2} \cdot (m_t + m_p) \cdot (\tau \cdot \omega)^2 = \frac{1}{2} \cdot (J_m + (m_t + m_p) \cdot \tau^2) \cdot \omega^2 = \frac{1}{2} \cdot J^* \cdot \omega^2$$

$$D = \frac{1}{2} \cdot c_d \cdot (\tau \cdot \omega)^2 + \frac{1}{2} \cdot c_T \cdot \omega^2 = \frac{1}{2} \cdot (c_T + c_d \cdot \tau^2) \cdot \omega^2 = \frac{1}{2} \cdot c^* \cdot \omega^2$$

$$\delta L = C_m \cdot \delta \vartheta \Rightarrow J^* \cdot \dot{\omega} + c^* \cdot \omega = C_m$$

Neglecting L_a for now, we get that:

$$\begin{cases} C_m = k\psi \cdot i_a \\ v_a = R_a \cdot i_a + k\psi \cdot \omega \end{cases} \Rightarrow C_m = -\frac{(k\psi)^2}{R_a} \cdot \omega + \frac{k\psi}{R_a} \cdot v_a$$

$$J^* \cdot \dot{\omega} + \left(c^* + \frac{(k\psi)^2}{R_a}\right) \cdot \omega = \frac{k\psi}{R_a} \cdot v_a$$

Moreover, being a 1/3, 1/3, 1/3 motion law in speed, we get an acceleration gain in the reference signal based on h and t_f :

$$\bar{a} = \frac{9 \cdot h}{2 \cdot t_f^2}$$

Dividing by τ , we get the reference angular acceleration.

1) FF control logic.

variables: $Jx = J^*$, $cx = (c^* + \frac{(k\psi)^2}{R_a})$,
reference acceleration: $\text{omega_} = \bar{a}/\tau$

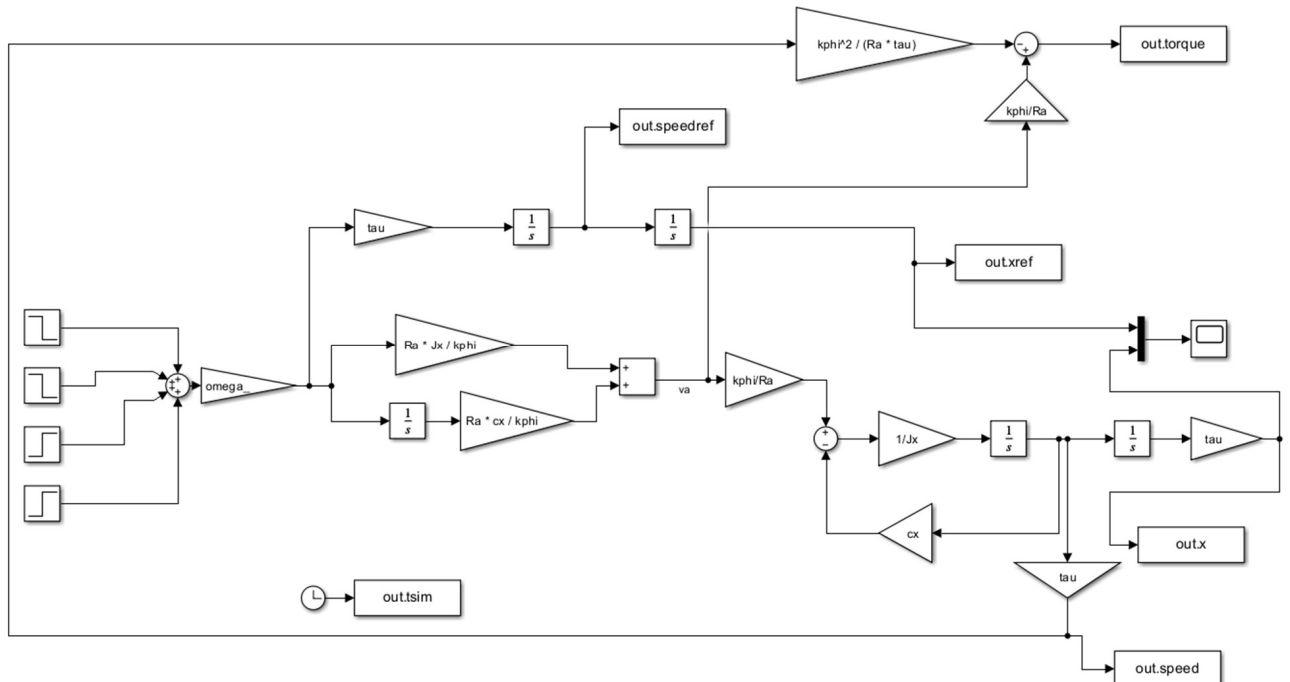


Figure 84: block diagram (case A1)

Defining the input signal as a superposition of step functions, we get that:

$$v_a = \frac{R_a \cdot J^*}{k\psi} \cdot \dot{\omega}_{ref} + \frac{R_a \cdot (c^* + \frac{(k\psi)^2}{R_a})}{k\psi} \cdot \omega_{ref}$$

Having no uncertainties in the parameters, we get speed and displacement. Reference and system's response are the same, meaning there are no discrepancies.

To compute the torque applied to the motor, we refer to the variables v_a and v , which is equal to:

$$v = \tau \cdot \omega$$

Thus:

$$C_m = -\frac{(k\psi)^2}{\tau \cdot R_a} \cdot v + \frac{k\psi}{R_a} \cdot v_a$$

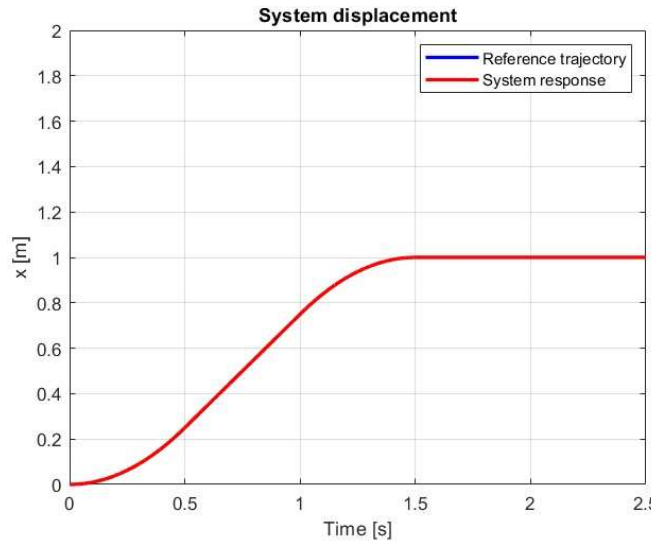


Figure 85: displacement (A1)

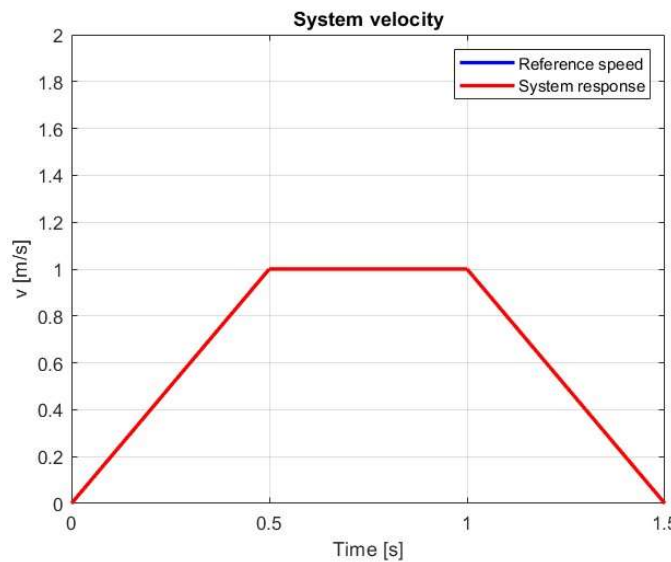


Figure 86: speed (A1)

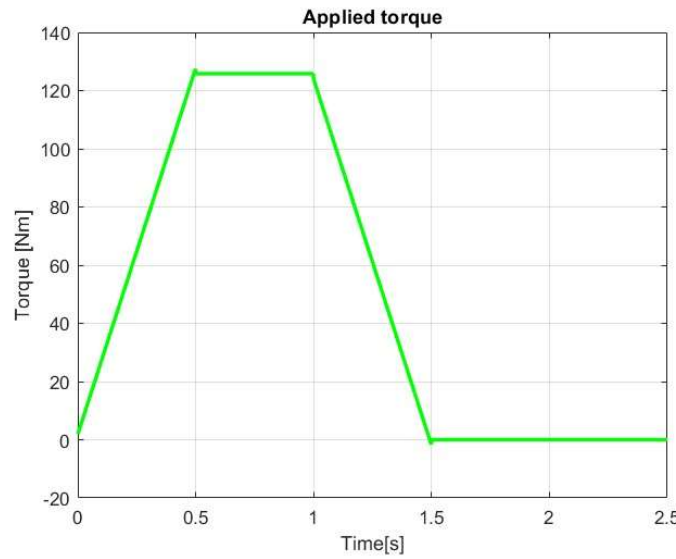


Figure 87: torque (A1)

2) FB control logic (P – control).

$$v_a = k_p \cdot (\omega_{ref} - \omega)$$

As an example, we choose $k_p = 50 \text{ Vs/rad}$. Here we show the block diagram, where variables are named as in the previous case and the subsystems represent the reference angular speed and the actual angular speed computation (given $\frac{k\psi}{R_a} \cdot v_a$) respectively.

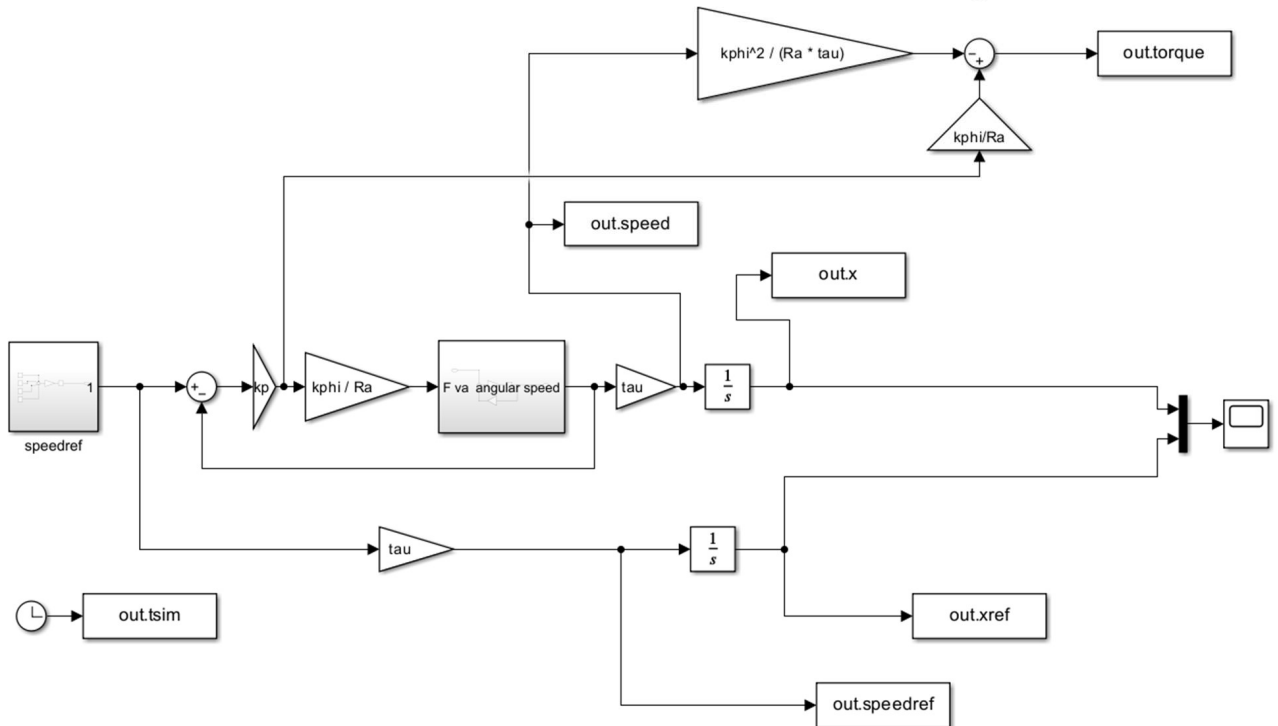


Figure 88: block diagram (case A2)

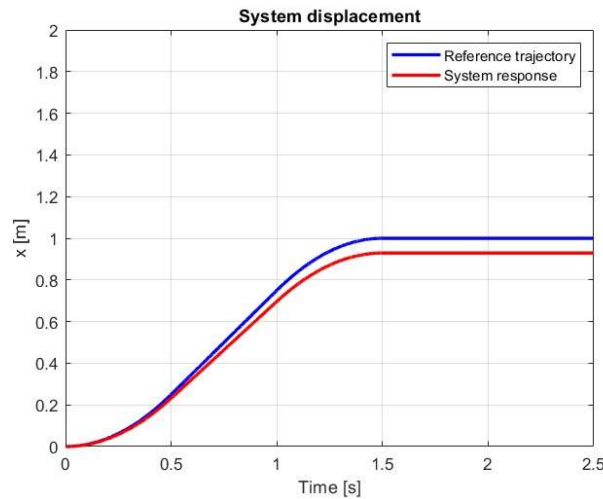


Figure 89: displacement (A2)

Steady-state error is not null here due to the presence of k_p . However, we could try with higher values of proportional gain to see that this discrepancy progressively decreases. The maximum torque is slightly lower than with FF control (there is lower tension, despite speed being lower too).

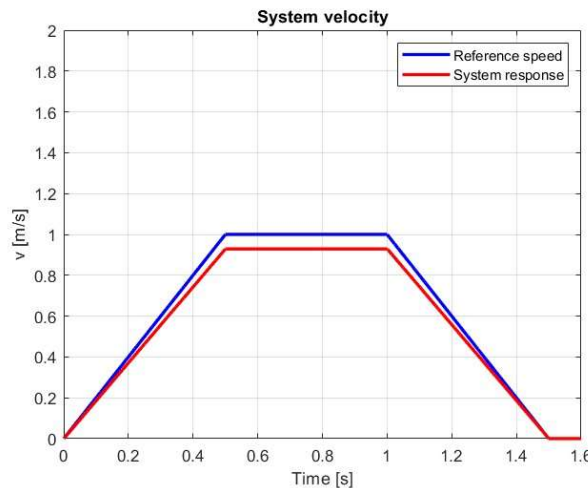


Figure 90: speed (A2)

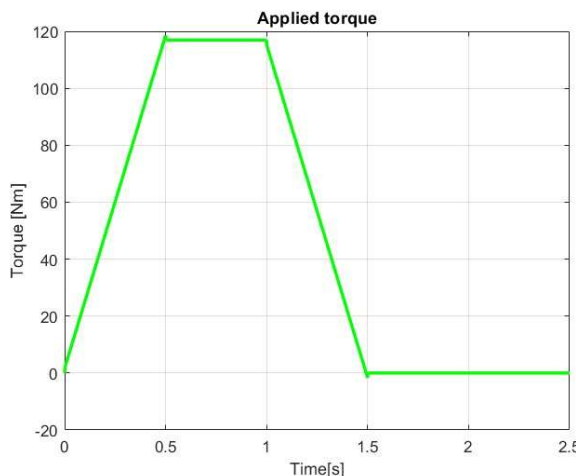


Figure 91: torque (A2)

3) FF control logic with uncertainties on system parameters.

We assume to increase both system equivalent parameters, with (as examples) $\Delta J^* = 0.003 \text{ kgm}^2$ and $\Delta c^* = 1 \text{ Nms/rad}$. It can be observed that final displacement is above the reference one, due to a higher voltage applied, and the same can be said for the maximum velocity. Moreover, despite a higher speed, an increase in the voltage leads to an overestimation of the torque that should be applied.

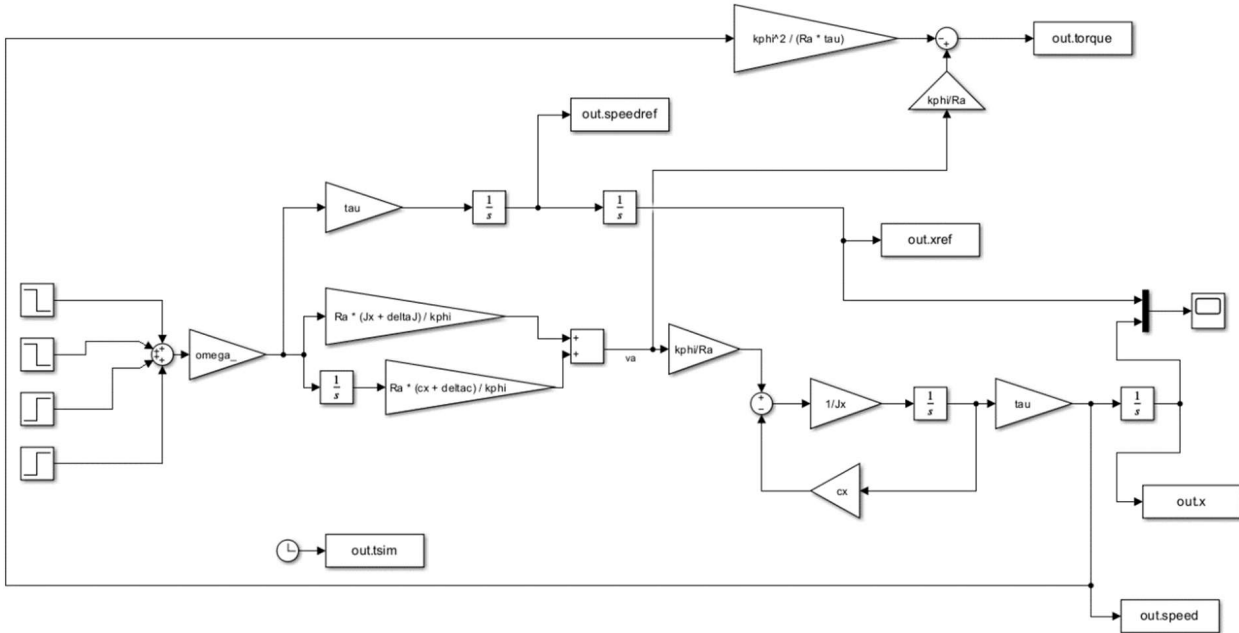


Figure 92: block diagram (case A3)

Difference with block diagram in *case A1* only lies in different values provided to the mathematical model. Note that differences must be added only when providing the modelled force, not even when control force acts on the real system.

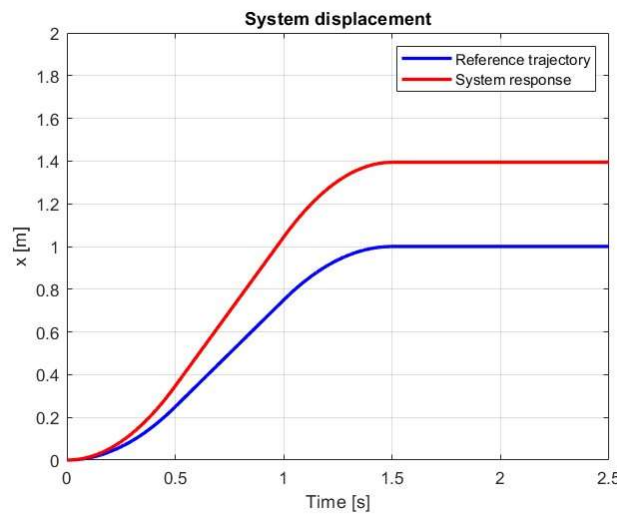


Figure 93: displacement (A3)

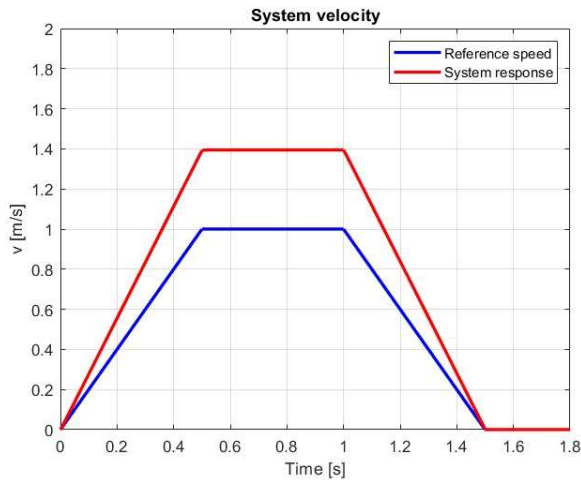


Figure 94: speed (A3)

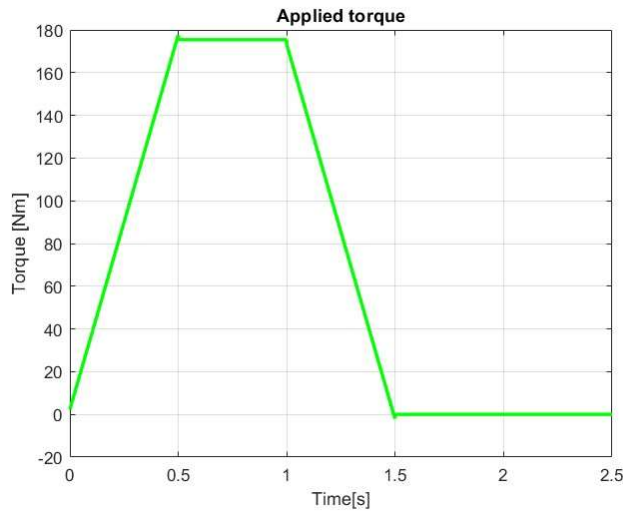


Figure 95: torque (A3)

4) Disturbance force applied on the machine table.

We introduce a random component on the tension input component.

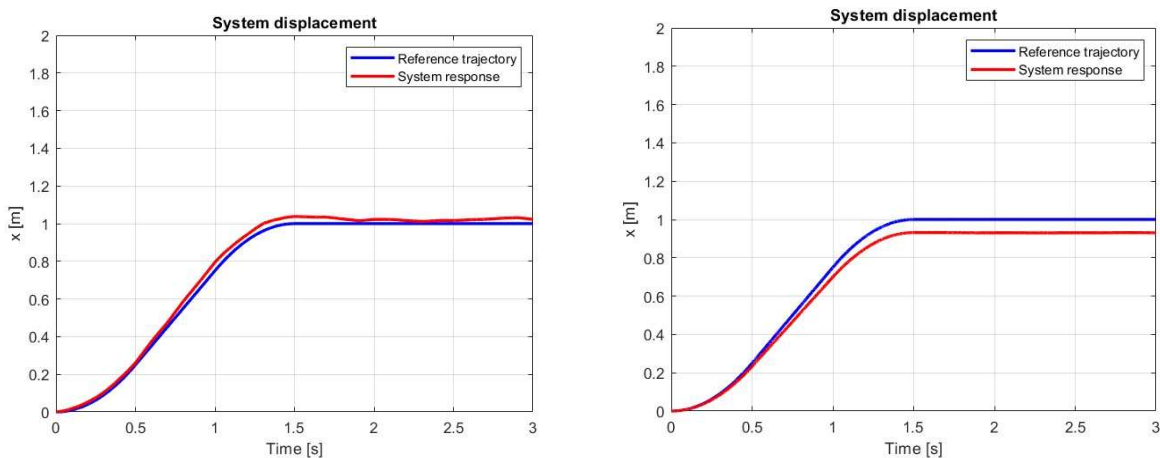


Figure 96: effect of disturbances on displacement (FF and FB)

The effect of disturbances on an FF control logic results in an irregular response, since there's nothing that can attenuate this behavior. On the other hand, the negative feedback mechanism (thanks to k_p) in the FB system damps disturbances.

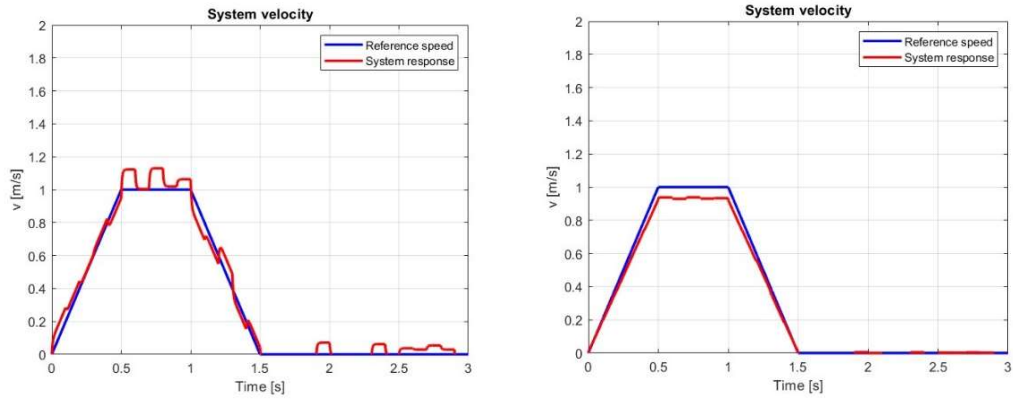


Figure 97: effect of disturbances on speed (FF and FB)

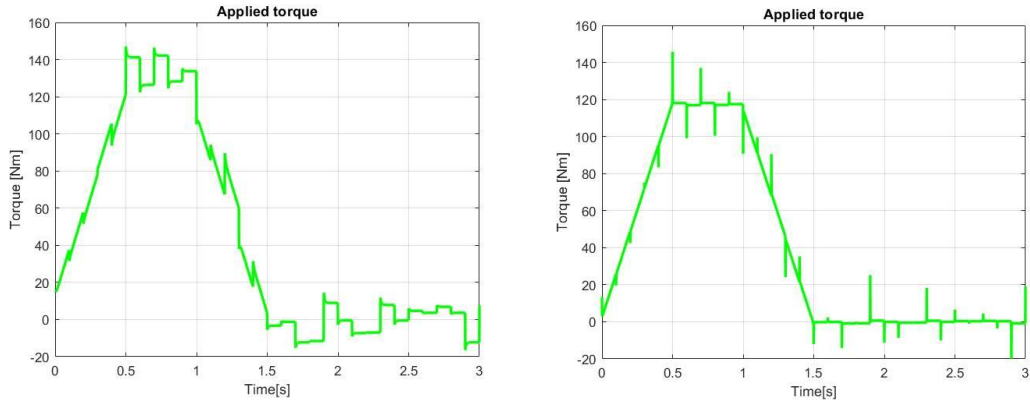


Figure 98: effect of disturbances on torque (FF and FB)

Block diagrams are simply modified by adding a random component to v_a .

5) Measurement noise in the FB control law.

The introduction of measurement noise changes the tension applied to the system, leading to random effects and irregularities in all the graphs. While disturbances could have been damped by increasing k_p , noise cannot be regulated this way.

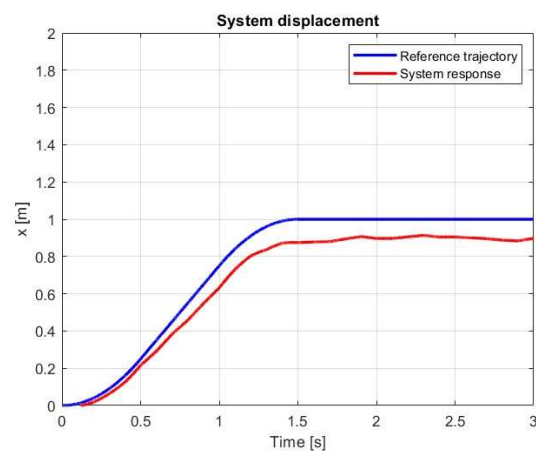


Figure 99: displacement (A5)

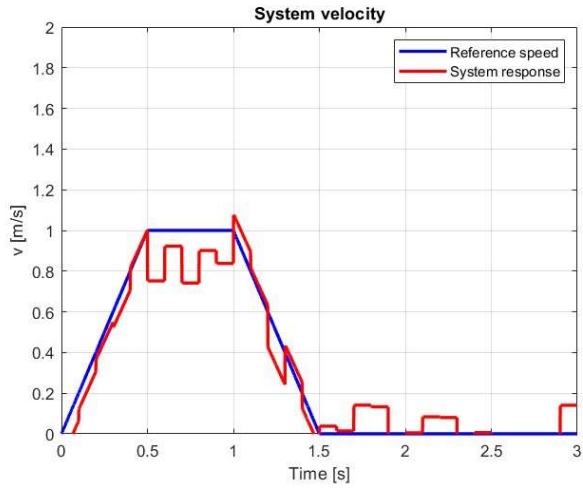


Figure 100: speed (A5)

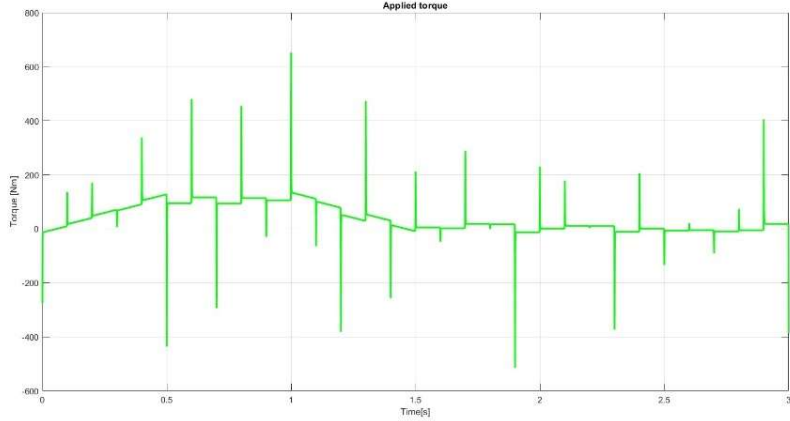


Figure 101: torque (A5)

The only ways to overcome this problem are to adopt the best possible measurement setup (sensors) or to use measurement *estimators* (based on a numerical-stochastic model).

3.2. CASE B: $L_a \neq 0, k_t \rightarrow \infty$.

We input to the system the tension input v_a computed in case A1, therefore considering the dynamics of the actuator as a model approximation. L_a cannot be neglected here; being the system:

$$\begin{cases} J^* \cdot \dot{\omega} + c^* \cdot \omega = C_m \\ C_m = k\psi \cdot i_a \\ v_a = R_a \cdot i_a + L_a \cdot \frac{di_a}{dt} + k\psi \cdot \omega \end{cases}$$

The equation of motion becomes:

$$J^* \cdot \dot{\omega} + (c^* + \frac{(k\psi)^2}{R_a}) \cdot \omega = \frac{k\psi}{R_a} \cdot v_a - \frac{L_a}{R_a} \cdot \frac{di_a}{dt} \cdot k\psi$$

1) FF control logic.

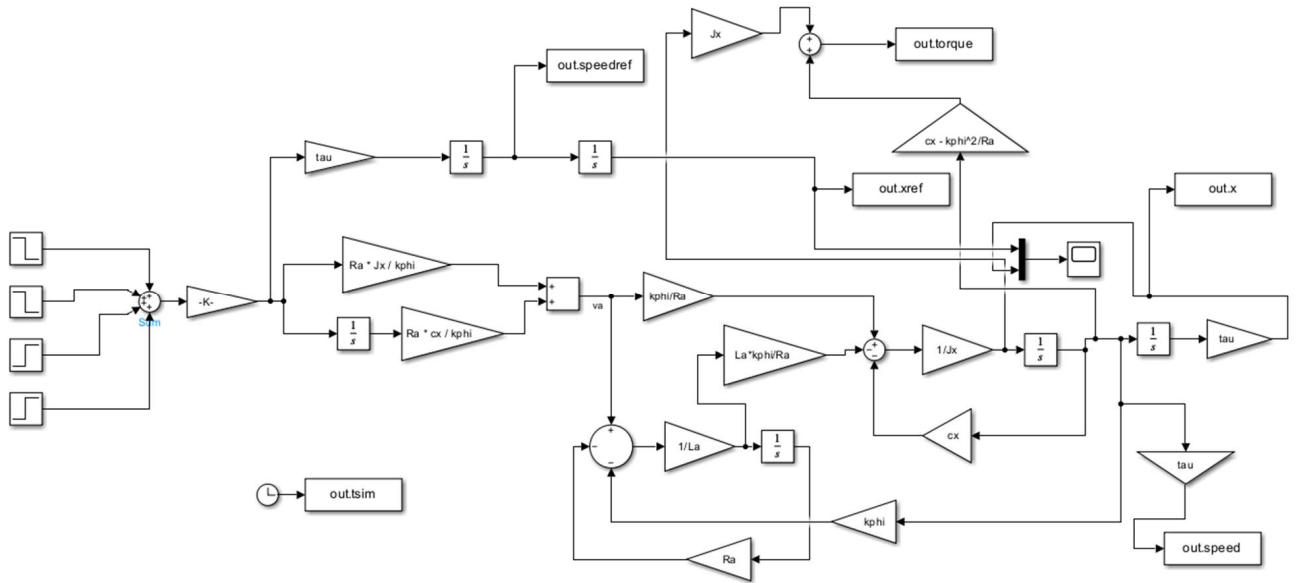


Figure 102: block diagram (B1)

The applied tension is the previous one (computed in the same way from the reference) while we also add the effect of current's time derivative to the control torque. This must be taken into account both when we describe the real system and when we compute the applied control torque too.

Results ($L_a = 0.008 \text{ H}$) are shown below:

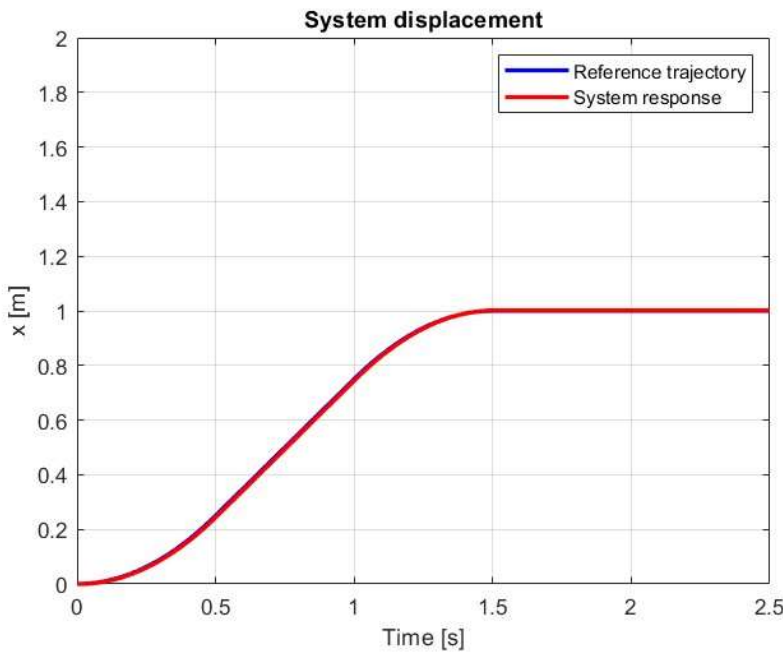


Figure 103: displacement (B1)

Note that the system is now second order, due to the introduction of L_a , and this results in a “delay” with respect to the reference. This is not so evident: the reason is that being the electrical system much faster than the mechanical one, we can neglect its dynamics in studying the motor.

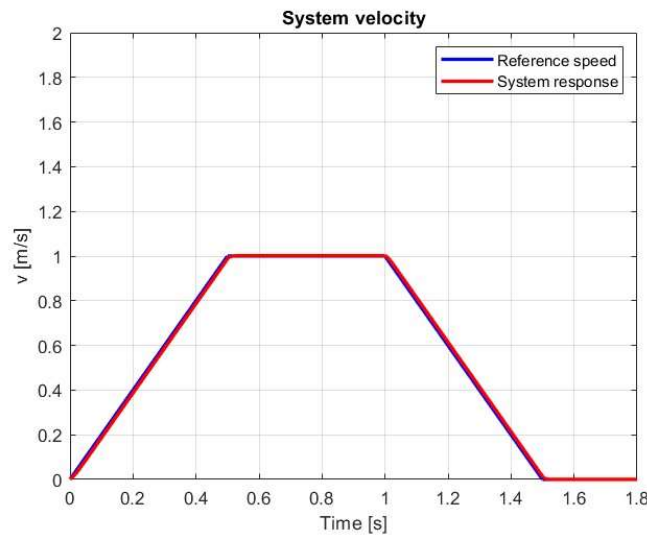


Figure 104: speed (B1)

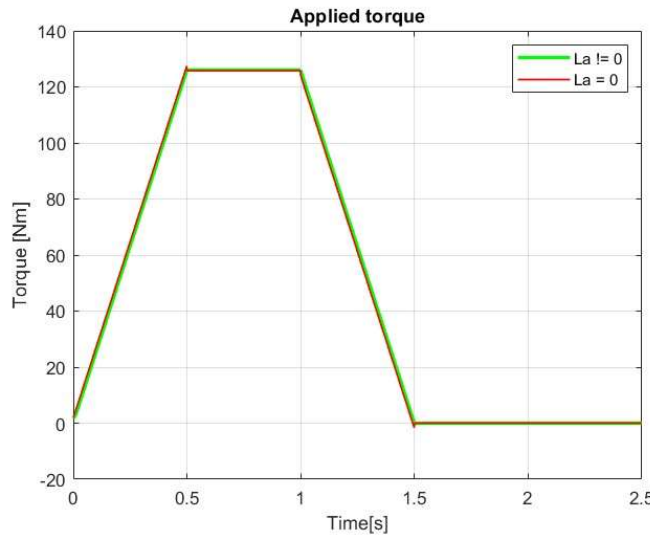


Figure 105: torque (B1)

Displacement and speed are (slightly, due to the low value of L_a) higher than the reference ones and moved to the right, and the same can be said for the torque. However, since L_a is almost negligible, the effect is not so evident; for instance, in case we increased tenfold L_a :

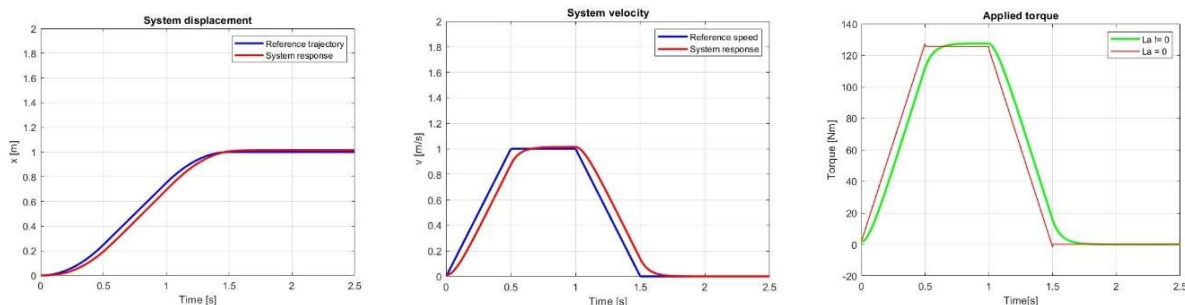


Figure 106: 10x L_a (B1)

The effect is much more evident.

2) FB control logic.

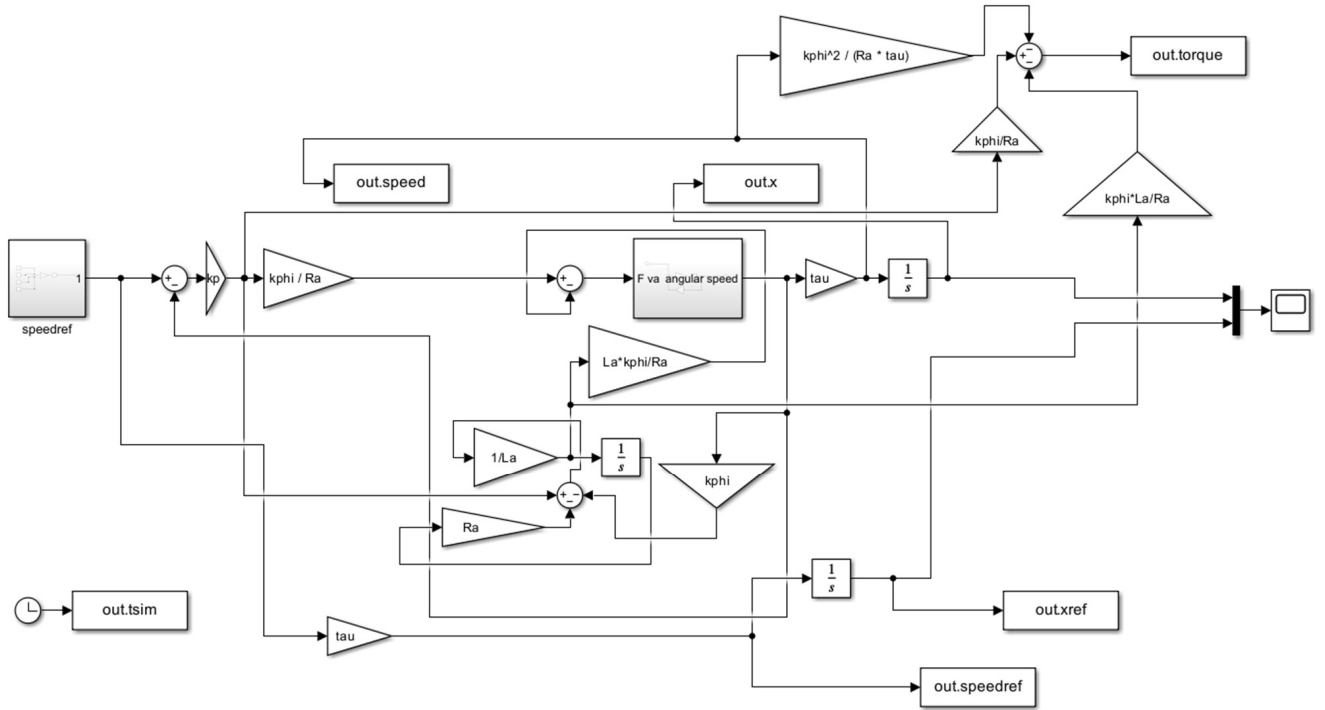


Figure 107: block diagram (B2)

Graphs are (slightly) moved to the right (always depending on the value of L_a), since they're second-order systems. However, final value only depends on k_p , while it is not affected by L_a ; it is shown in the graph below.

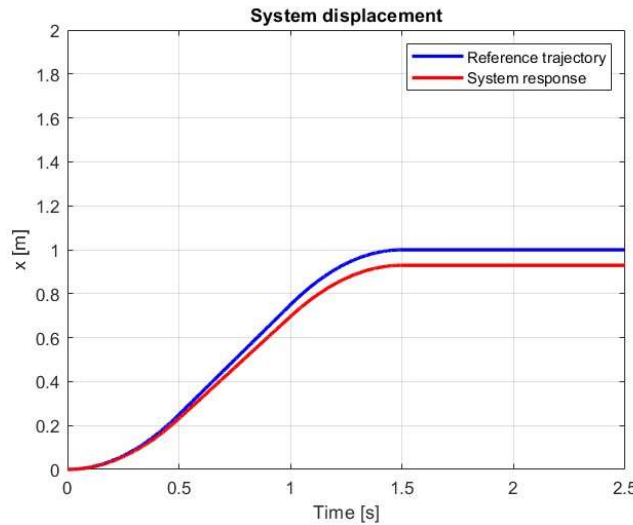


Figure 108: displacement (B2)

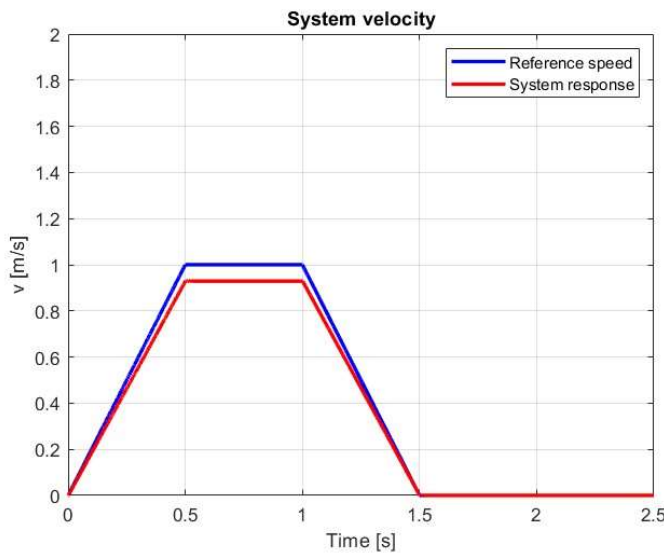


Figure 109: speed (B2)

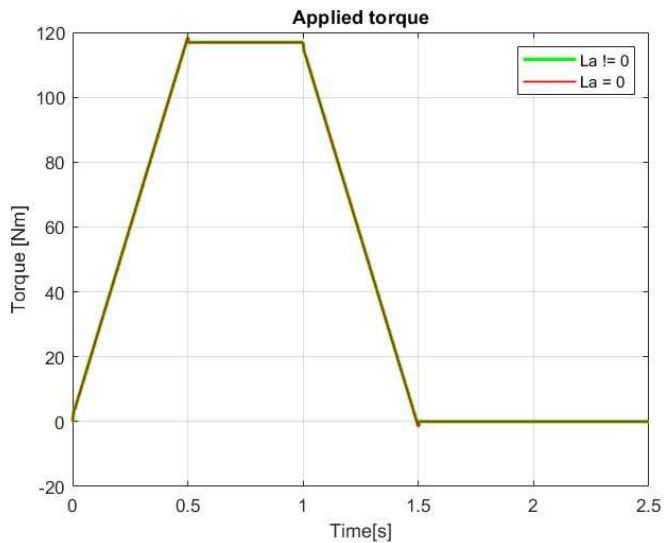


Figure 110: torque (B2)

If L_a is increased, the effect will be highlighted more. In this case, since it's less evident than in case B1, we decide to increase hundredfold L_a .

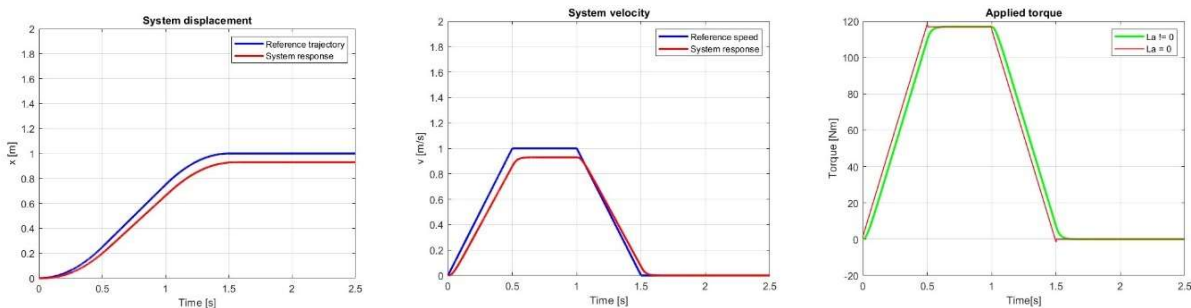


Figure 111: 100x L_a (B2)

3) FF with uncertainties on system parameters.

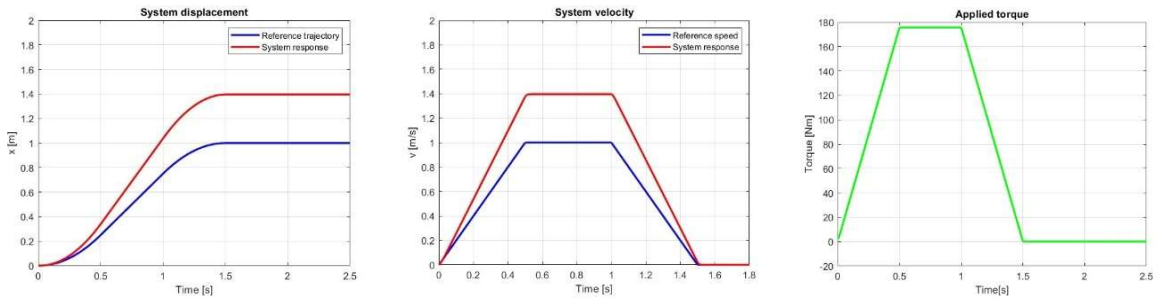


Figure 112: uncertainty on system parameters (B3)

Uncertainty has been introduced by adding arbitrary quantities (the same as in A3) to J^* and c^* . This results in an increase in displacement, speed and torque (and a shift caused by L_a). However, for this value of L_a the last effect is almost negligible.

4) Disturbance force applied on the machine table.

As seen in case A4, we can compare disturbances for both FF and FB control:

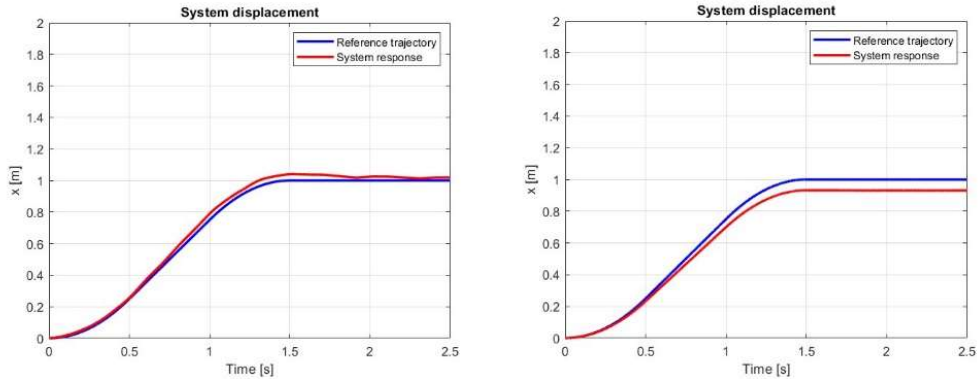


Figure 113: effect of disturbances on displacement (FF and FB)

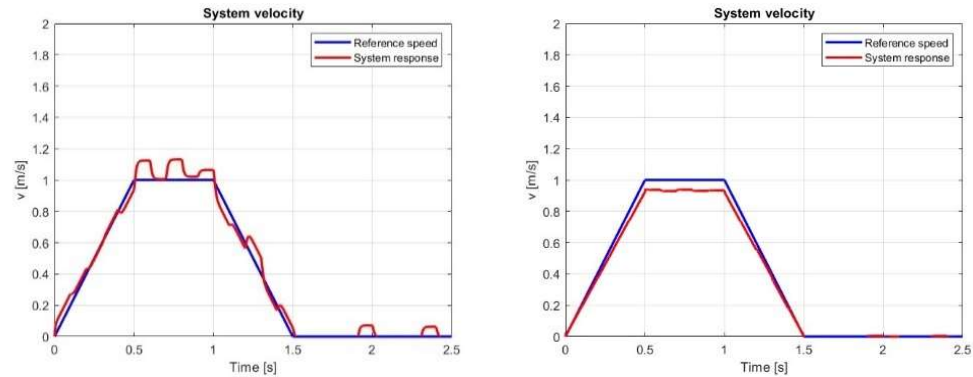


Figure 114: effect of disturbances on speed (FF and FB)

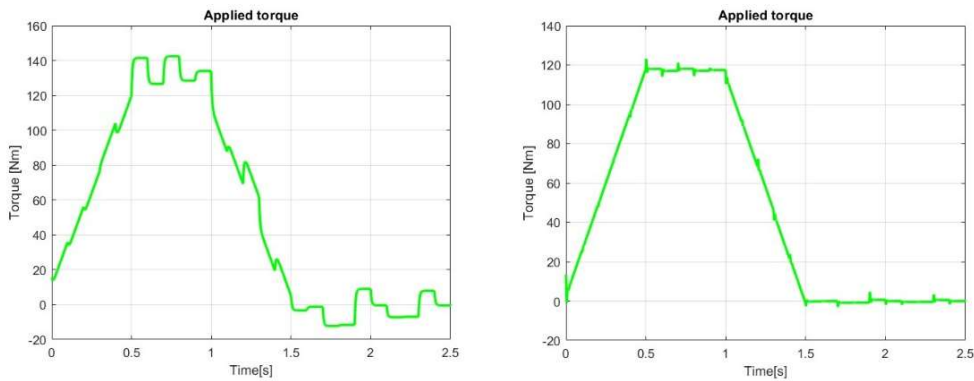


Figure 115: effect of disturbances on torque (FF and FB)

5) Measurement noise in the FB control law.

While disturbances could have been damped by increasing k_p , noise cannot be regulated this way. The result is shown below:

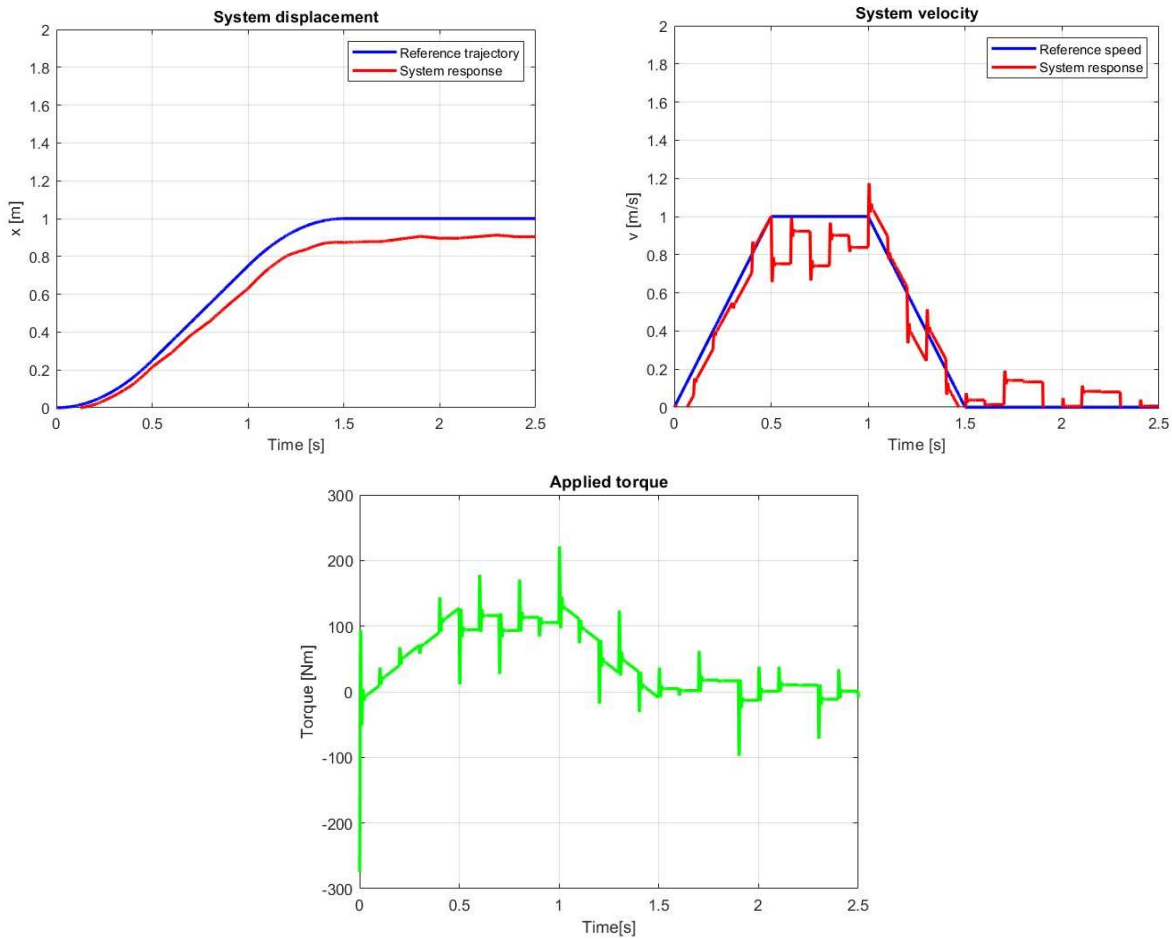


Figure 116: measurement noise in the FB control law (B5)

3.3. CASE C: $L_a = 0$, $k_t = 1000 \text{ Nm/rad}$.

Let's call ω_m the motor angular speed and ω_s the screw angular speed:

$$\begin{aligned}
E_c &= \frac{1}{2} \cdot J_m \cdot \dot{\theta}_m^2 + \frac{1}{2} \cdot (m_t + m_p) \cdot (\tau \cdot \dot{\theta}_s)^2 = \frac{1}{2} \cdot J_m \cdot \dot{\theta}_m^2 + \frac{1}{2} \cdot ((m_t + m_p) \cdot \tau^2) \cdot \dot{\theta}_s^2 \\
D &= \frac{1}{2} \cdot c_T \cdot \dot{\theta}_m^2 + \frac{1}{2} \cdot c_d \cdot (\tau \cdot \dot{\theta}_s)^2 = \frac{1}{2} \cdot c_T \cdot \dot{\theta}_m^2 + \frac{1}{2} \cdot (c_d \cdot \tau^2) \cdot \dot{\theta}_s^2 \\
V &= \frac{1}{2} \cdot k_T \cdot (\vartheta_m - \vartheta_s)^2 \\
\delta L &= C_m \cdot \delta \vartheta_m \\
\begin{cases} C_m = k\psi \cdot i_a \\ v_a = R_a \cdot i_a + k\psi \cdot \omega_m \end{cases} &\Rightarrow C_m = -\frac{(k\psi)^2}{R_a} \cdot \dot{\theta}_m + \frac{k\psi}{R_a} \cdot v_a \\
\begin{cases} J_m \cdot \ddot{\theta}_m + c_T \cdot \dot{\theta}_m + k_T \cdot (\theta_m - \delta \theta_s) = -\frac{(k\psi)^2}{R_a} \cdot \dot{\theta}_m + \frac{k\psi}{R_a} \cdot v_a \\ ((m_t + m_p) \cdot \tau^2) \cdot \ddot{\theta}_s + (c_d \cdot \tau^2) \cdot \dot{\theta}_s + k_T \cdot (\theta_s - \theta_m) = 0 \end{cases} \\
\begin{bmatrix} J_m & 0 \\ 0 & ((m_t + m_p) \cdot \tau^2) \end{bmatrix} \cdot \begin{pmatrix} \ddot{\theta}_m \\ \ddot{\theta}_s \end{pmatrix} + \begin{bmatrix} c_T + \frac{(k\psi)^2}{R_a} & 0 \\ 0 & (c_d \cdot \tau^2) \end{bmatrix} \cdot \begin{pmatrix} \dot{\theta}_m \\ \dot{\theta}_s \end{pmatrix} + \begin{bmatrix} k_T & -k_T \\ -k_T & k_T \end{bmatrix} \cdot \begin{pmatrix} \theta_m \\ \theta_s \end{pmatrix} \\
&= \begin{bmatrix} \frac{k\psi}{R_a} \\ 0 \end{bmatrix} \cdot v_a
\end{aligned}$$

In building the block diagrams, we can take advantage of the relations:

$$\begin{aligned}
\ddot{\vartheta}_m &= \frac{1}{J_m} \cdot \left(\frac{k\psi}{R_a} \cdot v_a - (c_T + \frac{(k\psi)^2}{R_a}) \cdot \dot{\vartheta}_m - k_T \cdot \theta_m + k_T \cdot \theta_s \right) \\
\ddot{\vartheta}_s &= \frac{1}{(m_t + m_p) \cdot \tau^2} \cdot (k_T \cdot \theta_m - c_d \cdot \tau^2 \cdot \dot{\vartheta}_s - k_T \cdot \theta_s) \\
C_m &= -\frac{(k\psi)^2}{R_a} \cdot \dot{\vartheta}_m + \frac{k\psi}{R_a} \cdot v_a
\end{aligned}$$

1) Co-located control.

$$v_a = k_p \cdot (\dot{\vartheta}_{ref} - \dot{\vartheta}_m)$$

From the stability analysis (e.g. Nyquist criterion) we know that the system is always stable whatever value of k_p we choose: this has already been shown numerically in assignment 2.

To show this phenomenon we use pre-defined values of k_p , ranging between 6 and 8 Vs/rad, which will be kept the same for the non-co-located control too.

$$\begin{cases} k_{p1} = 6 \text{ Vs/rad} \\ k_{p2} = 7 \text{ Vs/rad} \\ k_{p3} = 8 \text{ Vs/rad} \end{cases}$$

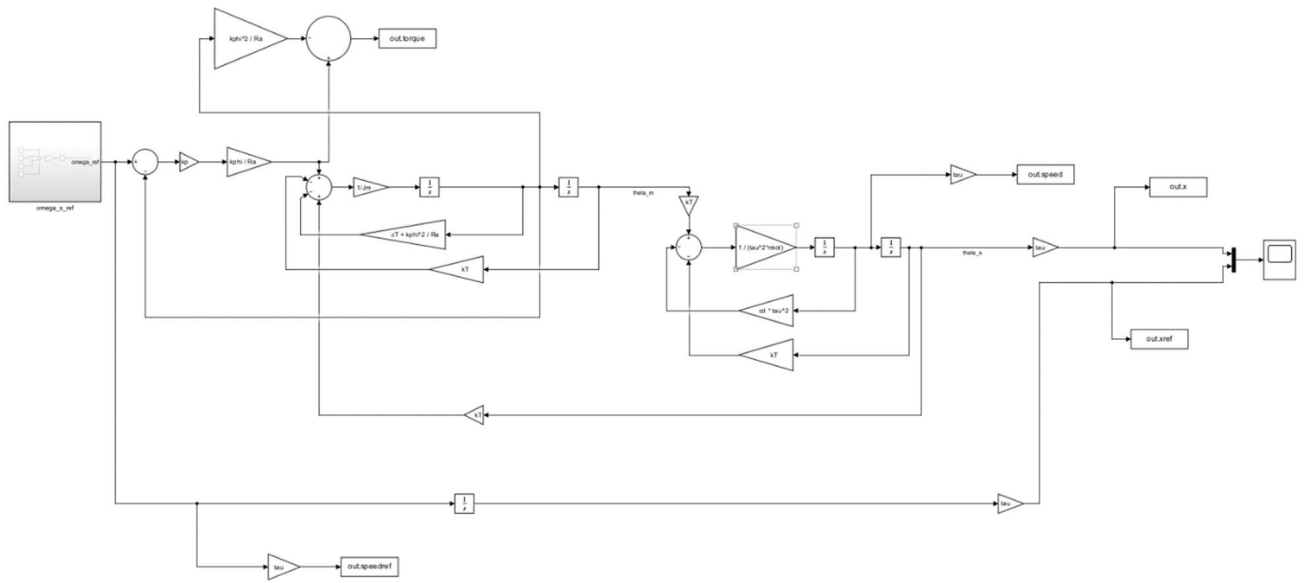


Figure 117: block diagram (C1)

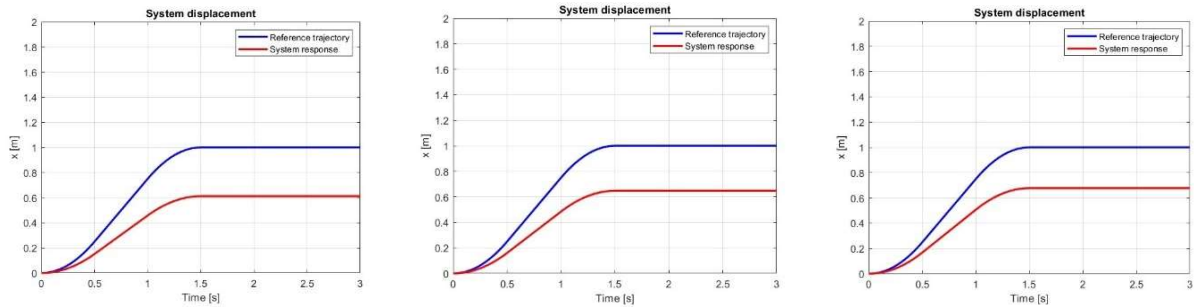


Figure 118: displacement (C1) for $k_p = 6, 7, 8$

As expected, steady-state error decreases for increasing values of k_p .

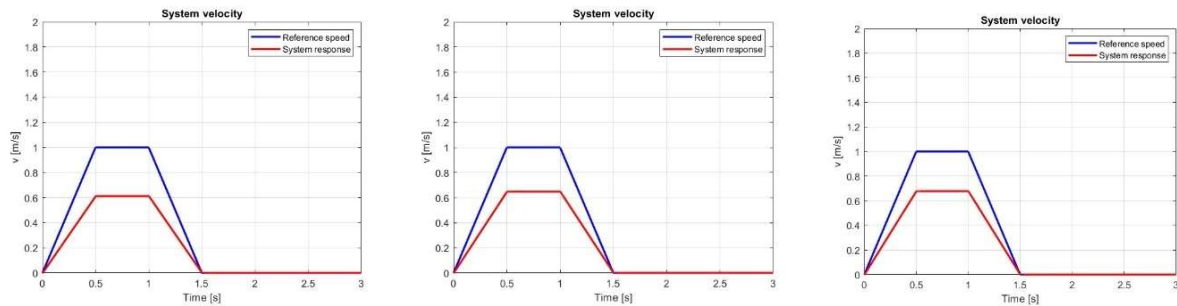


Figure 119: speed (C1) for $k_p = 6, 7, 8$

Speed increases, approaching the reference one, for increasing k_p .

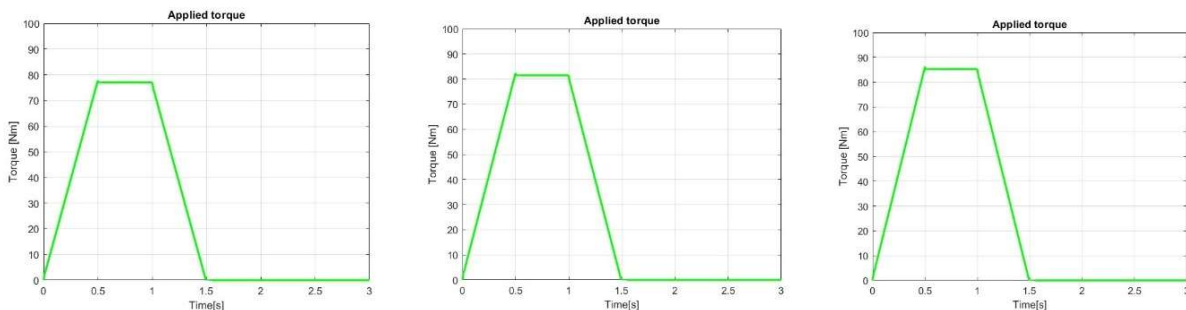


Figure 120: torque (C1) for $k_p = 6, 7, 8$

Torque also increases with the gain, due to higher values of v_a . In all cases system is stable, and this can be numerically verified with much higher values of k_p : for those the system's response almost overlaps with the reference one too.

2) Non-co-located control.

$$v_a = k_p \cdot (\dot{\vartheta}_{ref} - \dot{\vartheta}_s)$$

This way the positions of the actuator (electric motor) and the transducer (feedback signal and measurement) do not coincide. As seen in *assignment 2*, the system is not stable for high values of k_p , while it is for low ones. We define the same range of values as in *case C1* and see what happens.

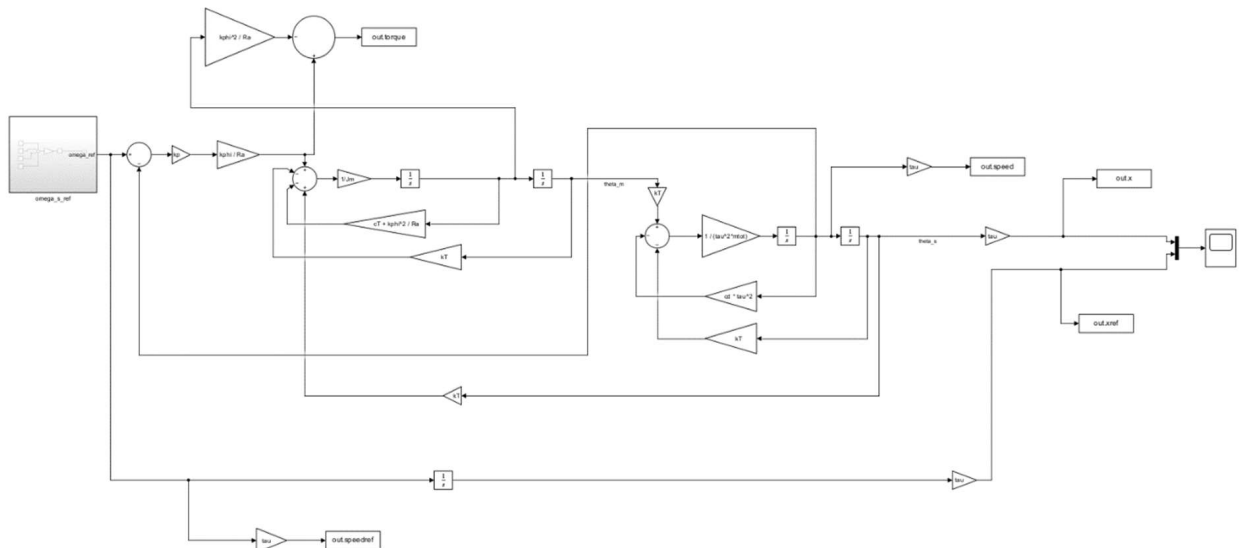


Figure 121: block diagram (C2)

The only difference between this block diagram and the previous one is that the definition of the tension v_a uses the screw angular speed instead of the motor one.

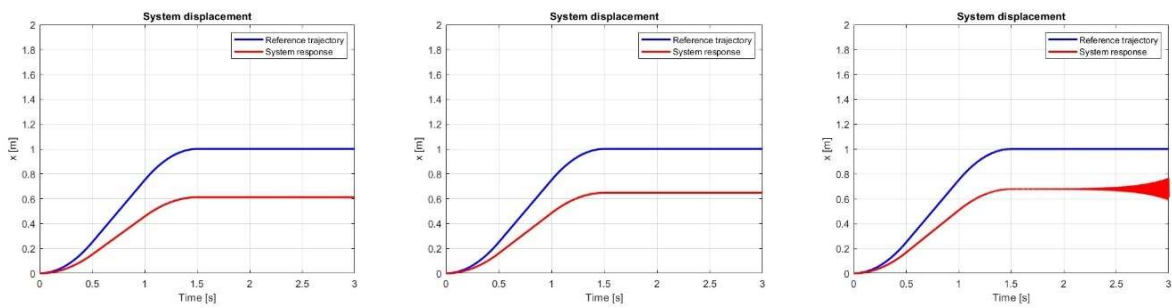


Figure 122: displacement (C2) for $k_p = 6, 7, 8$

For $k_p = 6, 7$ system remains stable, but for $k_p = 8$ it becomes unstable, with a response which will finally diverge. This phenomenon can be observed for speed and torque too.

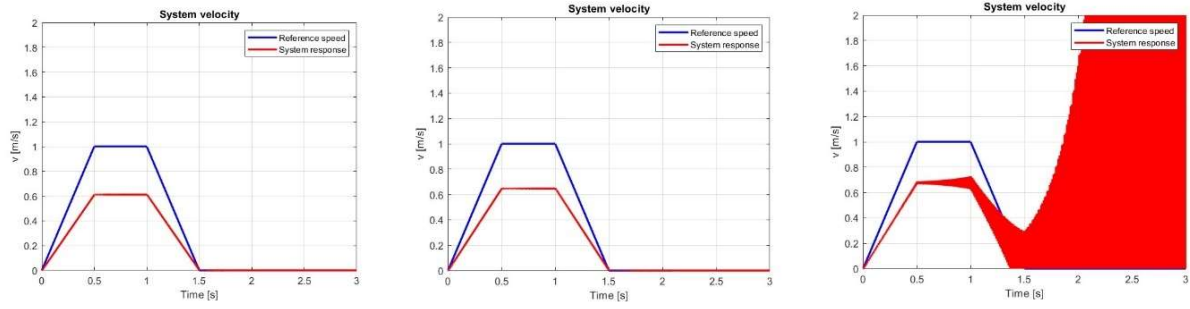


Figure 123: speed (C2) for $k_p = 6, 7, 8$

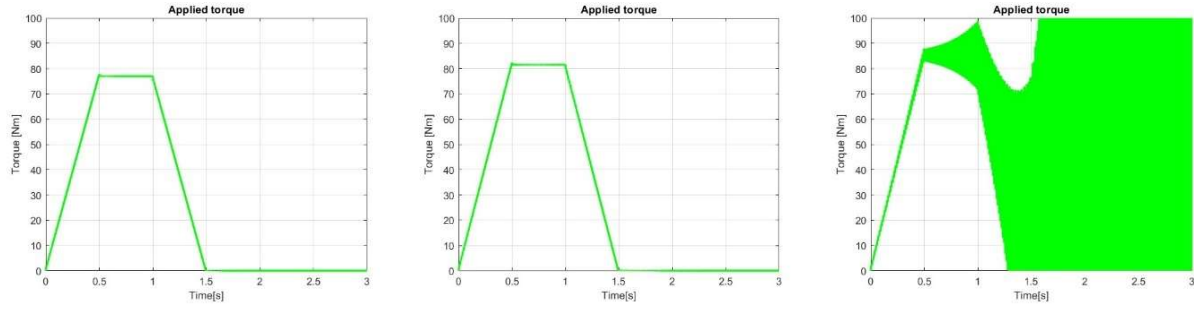


Figure 124: torque (C2) for $k_p = 6, 7, 8$

In conclusion, with a co-located control system is stable whatever gain we choose, while with a non-co-located one it becomes unstable for increasing gain.